CANCER

EpCAM-targeting CAR-T cell immunotherapy is safe and efficacious for epithelial tumors

Dan Li[1]†, Xianling Guo[2]†, Kun Yang[3]†, Yuening Yang[1], Weilin Zhou[1], Yong Huang[1], Xiao Liang[1,4], Jinhua Su[1], Lin Jiang[1], Jing Li[1], Maorong Fu[1], Haixia He[1,5,6], Jinrong Yang[1,7], Huashan Shi[1], Hanshuo Yang[1], Aiping Tong[1], Nianyong Chen[4]*, Jiankun Hu[3]*, Qing Xu[2]*, Yu-Quan Wei[1]*, Wei Wang[1]*

The efficacy of CAR-T cells for solid tumors is unsatisfactory. EpCAM is a biomarker of epithelial tumors, but the clinical feasibility of CAR-T therapy targeting EpCAM is lacking. Here, we report pre- and clinical investigations of EpCAM–CAR-T cells for solid tumors. We demonstrated that EpCAM–CAR-T cells costimulated by Dectin-1 exhibited robust antitumor activity without adverse effects in xenograft mouse models and EpCAM-humanized mice. Notably, in clinical trials for epithelial tumors (NCT02915445), 6 (50%) of the 12 enrolled patients experienced self-remitted grade 1/2 toxicities, 1 patient (8.3%) experienced reversible grade 3 leukopenia, and no higher-grade toxicity reported. Efficacy analysis determined two patients as partial response. Three patients showed >23 months of progression-free survival, among whom one patient experienced 2-year progress-free survival with detectable CAR-T cells 200 days after infusion. These data demonstrate the feasibility and tolerability of EpCAM–CAR-T therapy.

INTRODUCTION

Chimeric antigen receptor–modified T (CAR-T) cell therapy has been considered a new paradigm in the treatment of hematological malignancies due to remarkable clinical benefits and acceptable toxicity (*1*–*3*). Many researchers have attempted to repeat this success by eradicating solid tumors, but the results are far from satisfactory due to multiple challenges (*4*). One important hurdle is the lack of ideal target antigens. Target selection is pivotal for CAR-T immunotherapy, and the most ideal targets are tumor-specific antigens. However, potential antigens targeted by CAR-T therapy are not restricted to tumor cells, and they are also expressed on normal tissues, leading to lethal on-target/off-tumor toxicity to normal tissues (*5*, *6*). Therefore, comprehensive evaluation of the feasibility of CAR-T therapy targeting tumor-associated antigens (TAAs) is required before translating the therapy to clinical applications. Now, CAR-T therapies targeting TAAs, including disialoganglioside (GD2), human epidermal growth factor receptor 2 (HER2), and mesothelin, have been demonstrated to be tolerable in preclinical and clinical studies (*7*–*9*).

Epithelial cell adhesion molecule (EpCAM) is a transmembrane glycoprotein that is expressed in the epithelia and epithelial-derived neoplasms, including lung carcinoma, colorectal cancer, pancreatic cancer, and other epithelial tumors (*10*). Previous studies demonstrated that EpCAM was expressed on cancer stem cells and circulating tumor cells (CTCs) and was closely associated with tumor recurrence and metastasis (*11*, *12*), leading to the approval of EpCAM by the Food and Drug Administration as a diagnostic marker of CTCs of breast, prostate, and colorectal cancers (*13*). Many immunotherapies targeting EpCAM, including adecatumumab (anti-EpCAM), the trifunctional antibody catumaxomab (anti-EpCAM and anti-CD3), and oportuzumab monatox, have shown promising clinical benefits for patients with EpCAM-expressing tumors (*14*–*17*). It is therefore convincing to develop CAR-T therapy targeting EpCAM for the treatment of epithelial carcinomas. Although many preclinical investigations of EpCAM–CAR-T therapy have shown the inhibition of tumor growth and metastasis in animal models (*18*), clinical studies presenting detailed evaluations of the safety and efficacy of EpCAM–CAR-T therapy are lacking.

Here, in this study, we report the development of CAR-T therapy targeting EpCAM. We demonstrated that EpCAM–CAR-T cells showed robust antitumor efficacy with acceptable safety in immunodeficient mice and *EpCAM*-humanized immunocompetent mice. The pilot clinical studies we performed to evaluate the safety and efficacy of EpCAM–CAR-T cells (NCT02915445) for treating EpCAM-positive tumors demonstrated that systemic or peritoneal infusion of EpCAM–CAR-T cells was well tolerated without any target-directed toxicity. Two of 12 patients had a partial response to EpCAM–CAR-T therapy, and three patients had >23 months progress-free survival (PFS). This study demonstrated that EpCAM was feasible as a target for CAR-T therapy.

[1]Department of Biotherapy, State Key Laboratory of Biotherapy and Cancer Center, West China Hospital, Sichuan University, Chengdu, China. [2]Department of Oncology, Shanghai Tenth Peoples' Hospital, Shanghai, China. [3]Department of Gastrointestinal Surgery, West China Hospital, Sichuan University, Chengdu, China. [4]Department of Head and Neck Oncology, State Key Laboratory of Biotherapy and Cancer Center, West China Hospital, Sichuan University, Chengdu, China. [5]Guangdong Provincial Key Laboratory of Malignant Tumor Epigenetics and Gene Regulation, Medical Research Center, Sun Yat-Sen Memorial Hospital, Sun Yat-Sen University, Guangzhou, China. [6]Department of Radiation Oncology, Sun Yat-sen Memorial Hospital, Sun Yat-sen University, Guangzhou, China. [7]Department of Hematology, Hematology Research Laboratory, West China Hospital, Sichuan University, Chengdu, China.
*Corresponding author. Email: weiwang@scu.edu.cn (W.W.); hujkwch@126.com (J. H.); n_ychen@hotmail.com (N.C.); xuqingmd@tongji.edu.cn (Q.X.); yqwei@scu.edu.cn (Y.W.)
†These authors contributed equally to this work.

RESULTS

The intracellular domain of Dectin-1 as a suitable costimulatory domain for the CAR construct of CAR-T cells

Previous studies showed that antitumor efficacy benefited from costimulatory signaling (*19*, *20*). The various costimulatory domains endow CAR-T cells with different functions. The 4-1BB molecule enhanced the persistence of engineered lymphocytes (*21*, *22*). Some CAR-T cells containing the CD28 costimulatory domain showed an effective antitumor immune response in a short time (*23*, *24*). Dectin-1—as a non–Toll-like receptor pattern-recognition receptor that is widely expressed in dendritic cells, monocytes, neutrophils, and subpopulations of T cells—is considered a potential T cell function enhancer (*25*, *26*). In this study, we introduced Dectin-1, CD28, or 4-1BB costimulatory domains, which have been extensively examined in clinical studies, into EpCAM-CAR (CD28 CAR /4-1BB CAR /Dectin-1 CAR) and characterized the profile of these genetically engineered T cells (Fig. 1, A and B) and compared the Dectin-1 with CD28 and 4-1BB used in CAR to examine the features of CAR-T cells with different costimulatory domains. We first tested the differences in the effector functions of different CARs. The results of real-time cytotoxicity assay (RTCA) demonstrated that EpCAM-expressing tumor cells were eradicated by all CAR-T cells in the coculture system (fig. S1A). The cytotoxicity of Dectin-1 CAR-T cells to EpCAM-expressing tumor cells was similar to that of 4-1BB and CD28 CAR-T cells. Coincided with the antitumor effects, the cytotoxic effector molecules interferon-γ (IFN-γ) and interleukin-2 (IL-2) were equally secreted after CAR-T cells were activated by the EpCAM-positive cell lines HT-29 and SK-OV-3 (fig. S1B). Next, to investigate the difference of CD28, 4-1BB, or Dectin-1 costimulator-engaged CAR-T cells, we performed transcription profile analysis by RNA sequencing (RNA-seq). After 6 days of CAR modification, CAR-T cells were stimulated by plate-bounded EpCAM-Fc protein for 24 hours. And next, mRNA from CAR-T cells was extracted for sequencing. The cluster analysis demonstrated that Dectin-1 CAR-T cells showed similar cytokine and cytokine receptor gene signatures with 4-1BB CAR-T cells, while CD28 CAR-T cells showed higher enrichment of these genes in the transcription profile than the other two CAR-T cells (fig. S1C). Meanwhile, analysis of T cell exhaustion-related genes showed that the T cell hyporesponsiveness-related regulatory factor *NR4A1* (*27*) and the inhibitory molecule *CD200* (*28*) were elevated in CD28 CAR-T cells. In contrast, Dectin-1 and 4-1BB CAR-T cells had higher expression of the *JUN* and *FOSB* genes, which have been reported to induce exhaustion resistance (fig. S1D) (*28*, *29*). In addition, the results from gene set enrichment analysis (GSEA) demonstrated that Dectin-1 CAR-T cells showed enrichment of genes that contribute to central memory differentiation (fig. S1E), whereas genes related to down-regulate terminal effector differentiation were enriched in Dectin-1–based CAR-T cells in contrast to 4-1BB CAR-T cells (fig. S1F). These results suggest that all types of CAR-T cells have similar antitumor kinetics in vitro. Dectin-1– and 4-1BB–costimulated CAR-T cells might have lower immune activation and exhaustion-associated genes transcription. In contrast, CD28-stimulated CAR may transduce antigen-independent activation signaling, which has been shown to have tonic signaling transduction and result in CAR-T cell dysfunction in vivo (*30*). CAR-T cell anergy has been shown to be closely related to self-activation and early exhaustion, as well as resulting in antitumor efficacy limitations in vivo (*30*). To test the findings in gene enrichment and clarify the specific characteristics of Dectin-1–stimulated CAR-T cells, we compared Dectin-1 CAR-T cells to CD28 and 4-1BB CAR-T cells in many aspects. First, based on the findings in RNA-seq, three types of CAR-T cells were performed self-activation and early exhaustion analysis via flow cytometry after 9 days of expansion in vitro. The results demonstrated that Dectin-1 CAR-T cells retained expression of the costimulatory signals CD25, CD28, CD69, and CD127, which was similar to that of 4-1BB CAR-T cells and Mock-T cells (T cell transduced with empty lentivirus). In contrast, CD28 CAR-T cells had markedly elevated expression of the costimulatory signals CD25, CD28, and CD69 but reduced CD127 expression (Fig. 1, C and D). In addition, Dectin-1–based CAR-T cells displayed less early exhaustion confirmed by lower checkpoint receptors expression, especially that of TIM-3 and LAG-3 than CD28 CAR-T cells (Fig. 1E and fig. S1G). These results confirmed that Dectin-1 CAR-T cells have a quantitative decrease in early exhaustion and self-activation relative to CD28 CAR-T cells. Because tonic signaling transduction affects T cell differentiation, the results from GSEA predicted the differential expression of differentiation-related genes in various CAR-T cells. Therefore, we examined the differentiation of different CAR-T cells with flow cytometry. Different CAR-T cells were activated with plate-bound EpCAM-Fc protein. Three days later, CAR^+CD4^+ cells and CAR^+CD8^+ cells were gated for further analysis (fig. S2). In correspondence with the results from GSEA, Dectin-1 CAR-T cells retained a more central memory phenotype ($CD45RA^-CD62L^+$) than CD28 CAR-T cells and fewer terminal effector T cells ($CD45RA^+CD62L^-$) than 4-1BB CAR-T cells (Fig. 1F and fig. S1H). Previous research demonstrated that a memory phenotype is preferable to terminal differentiated effectors in adoptive therapy due to superior proliferation and persistence (*31*). A more central memory phenotype and fewer terminal effector phenotypes may benefit CAR-T cells that use Dectin-1 for costimulatory signaling. These results demonstrated that because Dectin-1 was associated with less exhaustion, more memory, and less terminal effector differentiation, it may be a promising costimulator for CARs in promoting T cell function.

Meanwhile, to exclude the effect from antigen dependence, we compared HER2-specific CAR-T cells costimulated with the three different intracellular domains (CD28, 4-1BB, and Dectin-1) (fig. S3A). Similar results were observed that Dectin-1 endows HER2–CAR-T cells with superior cytotoxicity (fig. S3, B and C), appropriate immune activation (fig. S3D), reduced exhaustion (fig. S3, E to G), and increased proportion of central memory phenotype differentiation (fig. S3, H to J). These findings suggested that Dectin-1 is a universal costimulatory domain for CAR-T cells.

An in vivo study was conducted to further validate the findings in vitro and understand the mechanism and kinetics of CD28-, 4-1BB–, and Dectin-1–stimulated CAR-T cells. NOD-*Prkdc*^{scid} *IL2rg*^{tm1}/Bcgen (B-NDG) mice were intraperitoneally inoculated with HT-29 tumor cells (day −7) that had been modified to stably express firefly luciferase (*Luc*). Mice treated with CD28, 4-1BB, or Dectin-1 stimulated EpCAM–CAR-T cells on days 0, 3, and 7, respectively (Fig. 1G). As shown, the majority of mice that were treated with different types of EpCAM–CAR-T cells showed tumor eradication (Fig. 1H), while two of the six mice that were treated with CD28 domain-containing EpCAM–CAR-T cells had tumor recurrence in a short time, and one mouse has experienced

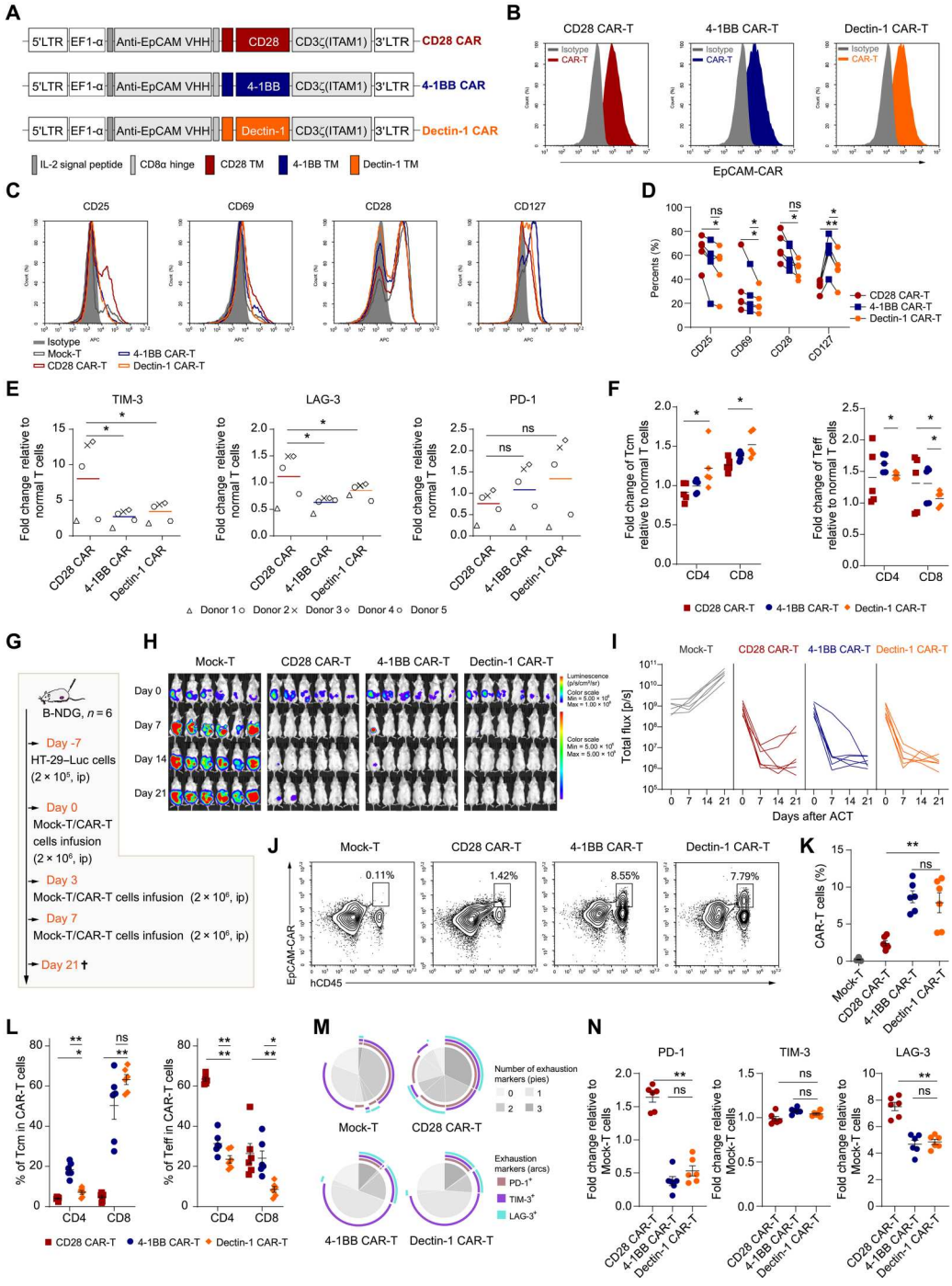

Fig. 1. The Dectin-1–stimulated EpCAM-specific CAR has a distinct effect on T cell in self-activation, differentiation, and exhaustion compared with that of CARs with the CD28 or 4-1BB costimulatory domain. (**A**) Schematic of EpCAM-specific CARs carrying CD28, 4-1BB, or Dectin-1 costimulatory domain. (**B**) Expression of different EpCAM-specific CARs on T cells, respectively. (**C** and **D**) Expression of activation-related markers on CAR-T cells after 9 days of CAR transduction. $n = 5$ different donors. Cells were pregated for the $CD3^+CAR^+$ subset. (**E**) Expression of exhaustion-associated receptors on CAR-T cells after 9 days of lentivirus transduction. The color lines are represented as mean. (**F**) Fold change of EpCAM–CAR-T cells differentiation in central memory and effector phenotypes of five different donors. The data are displayed as mean. (**G**) Schematic of the xenograft model. B-NDG mice were intraperitoneally injected with 2×10^5 HT-29–Luc cells on day −7. After that, the mice were intraperitoneally infused with three doses of Mock-T or CAR-T cells. $n = 6$ mice for each group. After 21 days of tumor inoculation, mice were euthanized to analyze CAR-T cell persistence. (**H** and **I**) Bioluminescence images and statistical results of tumor burden. (**J** and **K**) The percent of splenetic Mock-T cells and CAR-T cells after 21 days of adoptive T cell therapy. (**L**) Differentiation of splenetic $CD4^+$ and $CD8^+$ CAR-T cells in central memory and effector phenotypes in the xenograft model. (**M** and **N**) Exhaustion-associated receptors expression on splenetic CAR-T cells after 21 days of adoptively T cells administration. The data are presented as mean ± SD. *$P < 0.05$ and **$P < 0.01$. $P < 0.05$ was considered statistically significant. ns, no significance. Wilcoxon test was used for (D) to (F). Two-tailed unpaired Student's t test was used for differences analysis in (K), (L), and (N). TM, transmembrane domain; Teff, effector T cell; Tcm, central memory T cells.

delayed tumor regression after receiving 4-1BB CAR-T cell administration (Fig. 1, H and I). The effective homing and enhanced persistence have contributed to the sustained tumor clearance activity of Dectin-1– and 4-1BB–containing EpCAM–CAR-T cells (Fig. 1, J and K). The sustained persistence of Dectin-1 and 4-1BB CAR-T cells was ascribed to more proportion of central memory phenotype and less terminal effector phenotype (Fig. 1L and fig. S1I). Dectin-1 CAR-T cells have displayed lower exhaustion-associated surface markers expression, including programmed cell death protein 1 (PD-1) and LAG-3, which was consistent with 4-1BB CAR-T cells (Fig. 1, M and N, and fig. S1J). Combined the findings in vitro and in vivo, we confirmed that Dectin-1 promotes CAR-T cells function by increasing memory differentiation, resistance to exhaustion, and decreasing terminal effector phenotype, which may benefit CAR-T cells' persistence and survival in vivo.

Considering the priorities found above, we determine to costimulate CAR-T cells with the intracellular domain of Dectin-1. Therefrom, in all of the following experiments in this study,

CAR-T cells with the specificity to EpCAM were stimulated by Dectin-1intracellular domain and henceforth named as EpCAM–CAR-T cells.

Intraperitoneal and intravenous infusion of EpCAM–CAR-T cells

Given the observed characteristics of Dectin-1–costimulated EpCAM–CAR-T cells in vitro and in vivo and the exquisite antigen density-sensitive recognition (fig. S4, A to D) and antigen density-dependent cytotoxicity for tumor cells (fig. S4, E and F), we thought that it is necessary to further evaluate the effect of antitumor efficacy on different therapeutic doses and CAR-T cells delivery methods with xenograft tumor models. B-NDG mice were intraperitoneally inoculated with HT-29–Luc tumor cells. These tumor-bearing mice received triple EpCAM–CAR-T cell infusions intravenously or intraperitoneally after 7, 10, and 14 days of tumor cell inoculation (Fig. 2A). Tumor burden was monitored by bioluminescence imaging (BLI). Intravenous infusion of 1×10^7 CAR-T cells mediated complete tumor regression within 2 weeks (Fig. 2, B and C). A lower dose (2×10^6 cells) was effective in delaying tumor growth, and mice treated with Mock-T cells underwent rapid tumor progression and were euthanized within 4 weeks (Fig. 2, B to D). Compared with those in the Mock-T cell treatment group, the mice that received CAR-T cells achieved remarkable survival benefits (Fig. 2E). Peritoneal infusion of CAR-T cells resulted in more rapid and robust tumor eradication than intravenously infused CAR-T cells (Fig. 2, F to H). Compared with intravenous infusion, mice that received peritoneally infused CAR-T cells had a longer survival period (Fig. 2I) and more rapid recovery of body weight (fig. S5, A and B). At the end point of the experiment (above 40 days after CAR-T cells infusion), tumors relapsed and reduced survival in the lower dose (2×10^6 cells) treated group in both intraperitoneal and intravenous treatment models, especially in mice with the intravenous treatment group. That ascribe lower CAR-T cells homing and poor infiltration in tumors. The efficacy of EpCAM–CAR-T cells was closely related to highly efficient spleen homing and sustained persistence (above 40 days) in both the peritoneal and intravenous infusion groups (Fig. 2, J to M). In mice that received intravenous infusion, EpCAM–CAR-T cells were detected in peripheral blood at low levels 40 days after infusion (Fig. 2, N and O). In the high-dose group, the antitumor efficacy could be attributed to successful CAR-T cells infiltration into the tumor tissues because more CAR-T cells were detected in the tumor tissue in the high-dose group than in the low-dose group (Fig. 2, P and Q).

Moreover, the safety of EpCAM–CAR-T cell therapy was preliminarily evaluated. After EpCAM–CAR-T cell infusion, there were no obvious treatment-related adverse effects in response to intravenous or peritoneal infusion (fig. S5, A and B). Haematoxylin and eosin (H&E) staining of tissues showed no pathological signs of tissue damage in the low- or high-dose peritoneal and intravenous infusion groups (fig. S5, C and D). These results demonstrated that different therapeutic doses and local or systemic delivery of EpCAM–CAR-T cells was well tolerated by mice, and further investigating the clinical benefits would be feasible and valuable.

Safety of EpCAM–CAR-T cells in EpCAM-humanized mice

Although the immunodeficient xenograft mouse model is widely used to evaluate the efficacy of CAR-T therapy, it poorly predicts treatment-related clinical toxicities because these mice lack the same antigen that is targeted by CAR-T cells and bystander immune cells and reject human cell engraftment (*32*). To reliably investigate the safety of EpCAM–CAR-T cells, we designed *EpCAM*-humanized C57BL/6 (C57BL/6-*EpCAM*$^{tml\ EpCAM}$) mice. The mouse *EpCAM* gene locus was truncated, and the homologous human *EpCAM* gene locus was inserted by the CRISPR-Cas9 system (Fig. 3A). Pathological analysis showed that there was no evidence of abnormalities in the major organs of genetically engineered mice compared with wild-type mice (fig. S6A). The membrane biodistribution of human EpCAM in murine tissue was mainly in the epithelium of the alimentary canal and nephric tubule, skin, and pulmonary alveoli (fig. S6B), which was consistent with that in human tissues (fig. S7, A and B).

To further examine the potential toxicity of EpCAM–CAR-T cells in vivo, C57BL/6-*EpCAM*$^{tml\ EpCAM}$ mice were treated with cyclophosphamide (100 mg/kg) for lymphodepletion. After 2 days, three different doses of murine CAR-T cells targeting human EpCAM (1×10^6, 5×10^6, and 1×10^7) were intravenously infused into the different groups. Mice that were treated with Mock-T cells were used as control (Fig. 3B). After T cell treatment, there was no obvious change in body weight in the different treatment groups, even in response to the high dose of CAR-T cells (Fig. 3C). Cytokine release syndrome (CRS) is a critical clinical sign of excessive T cell activation and proinflammatory cytokine production and is a key predictor of fatal adverse events in T cell therapy (*33*). There was no typical cytokine release after administration of CAR-T cells, except IFN-γ, which increased slightly (Fig. 3D). In addition, the penetration of the infused T cells was evaluated. A previous study demonstrated that systemically infused CAR-T cells accumulated in the lung, liver, and other critical organs and resulted in on-target/off-tumor toxicity (*34*). In this study, the infused CAR-T cells prominently accumulated in the spleen and lung but not in the liver (Fig. 3, E and F). The number of infiltrated T cells in the organs positively correlated with the infusion dose (Fig. 3, E and F). In organs where EpCAM is expressed at low levels, including the colon, intestine, skin, and lung, few EpCAM–CAR-T cells were detected by specific CD3 staining (Fig. 3E) or CAR gene detection (Fig. 3F). Moreover, no evidence of inflammation, necrosis, or other pathological damage was detected in the heart, liver, spleen, lung, kidney, or other main organs in mice that received adoptive T cell therapy (Fig. 3, G to J, and fig. S8).

Further, safety study of EpCAM–CAR-T therapy in tumor-bearing EpCAM-humanized mice was performed to confirm the feasibility of this therapy. To evaluate the antitumor activity of EpCAM–CAR-T cells in EpCAM-humanized mice, B16-EpCAM-Luc cells were subcutaneously inoculated in EpCAM-humanized mice on day −3, and then the mice were subsequentially treated with 1×10^7 EpCAM–CAR-T cells or Mock-T cells on days 0, 3, and 7 (fig. S9A). As expected, EpCAM–CAR-T cells inhibited tumor growth effectively (fig. S9, B and C) and prolonged survival of mice (fig. S9D). Meanwhile, EpCAM–CAR-T cells were well tolerated by mice with unobvious body mass and body temperature change (fig. S10, A and B). There was no organ damage evidence according to blood biochemistry analysis (fig. S10, C to F) and pathological analysis (fig. S10G).

These results indicated that adoptively transferred EpCAM–CAR-T cells were tolerable in EpCAM-humanized mice and predicted the safety of EpCAM–CAR-T cell therapy in humans because EpCAM has a similar expression pattern in mice and

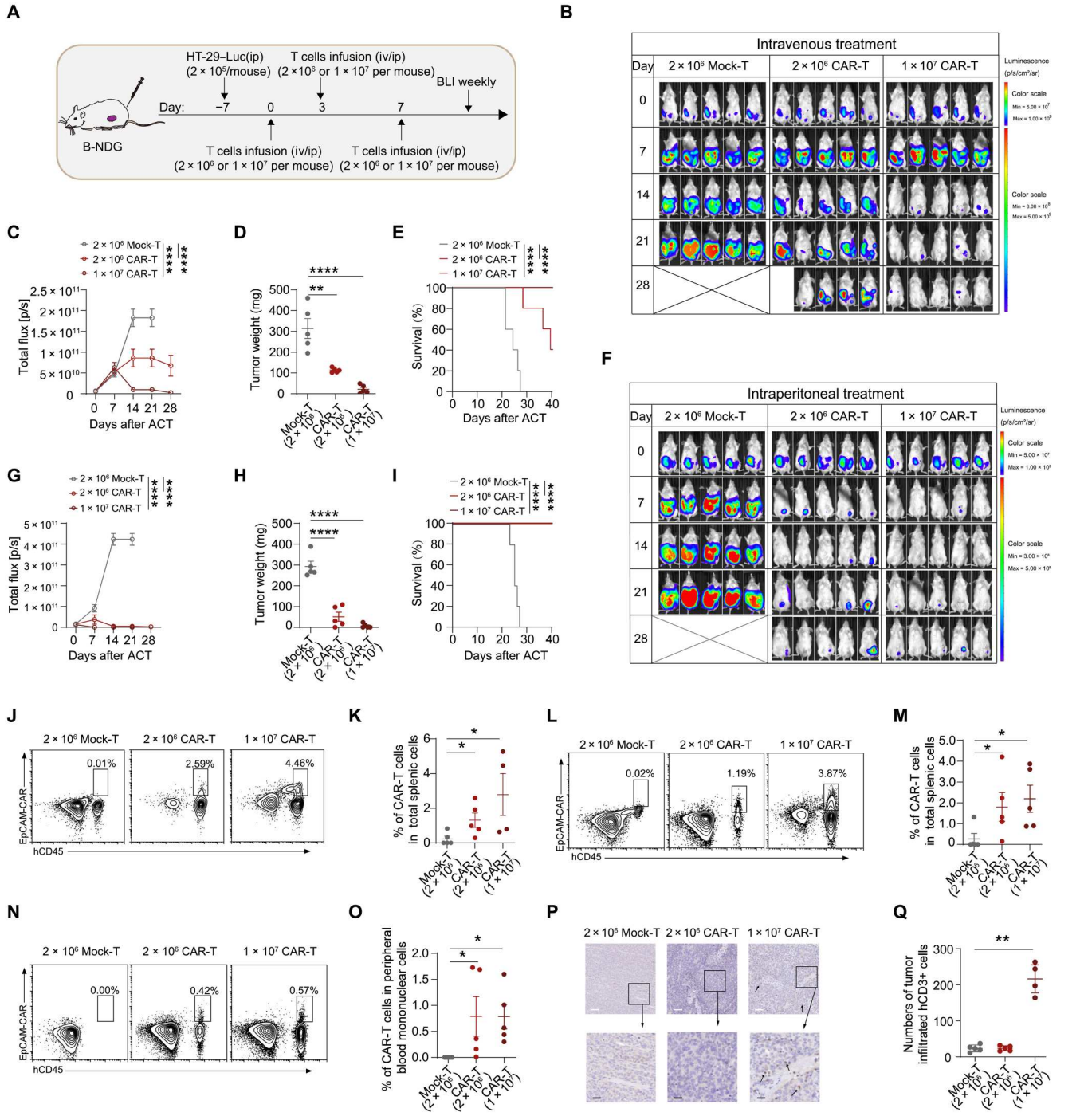

Fig. 2. Intraperitoneal and intravenous infusion of EpCAM–CAR-T cells induced colon cancer remission in a xenograft mouse model. (**A**) Schematic of the animal experiments. B-NDG mice were intraperitoneally injected with 2×10^5 Luc-expressing HT-29–Luc cells on day −7. After that, the mice were randomly assigned to different groups and were intraperitoneally or intravenously infused with three doses of Mock-T or CAR-T cells. $n = 5$ mice for each group. (**B** and **C**) Bioluminescence images and statistical result of tumor burden after intravenous administration of CAR-T cells. (**D** and **E**) Tumor weight at the end point of the experiment and the survival of mice who received intravenous CAR-T infusion. (**F** and **G**) Bioluminescence images and statistical result of tumor burden after intraperitoneal administration of CAR-T cells. (**H** and **I**) Tumor weight at the end point of the experiment and the survival of mice who received intraperitoneal CAR-T infusion. (**J** to **M**) Flow cytometry analysis of EpCAM–CAR-T cell persistence in the spleens of mice with intravenous (J) and (K) or intraperitoneal (L) and (M) T cell infusion. The Mock-T cell group was examined on day 21, and the CAR-T cell groups were examined when euthanized. $n = 4$ mice in the 1×10^7 CAR-T cells intravenously treated group and $n = 5$ mice in the other group. (**N** and **O**) EpCAM–CAR-T cells persisted in the peripheral blood of mice that received intravenous infusion of T cells. (**P** and **Q**) Representative results showing tumor-infiltrated human $CD3^+$ T cells in mice that received intravenous injection of T cells, as determined by immunohistochemistry (P) and statistical results shown in (Q). Scale bars, 200 μm (white) and 50 μm (black). The data are expressed as the means ± SD. Log-rank test for (E) and (I) and Mann-Whitney *U* test for (C), (D), (G), (H), (K), (M), and (O). $^*P < 0.05$, $^{**}P < 0.01$, and $^{****}P < 0.0001$. $P < 0.05$ was considered statistically significant.

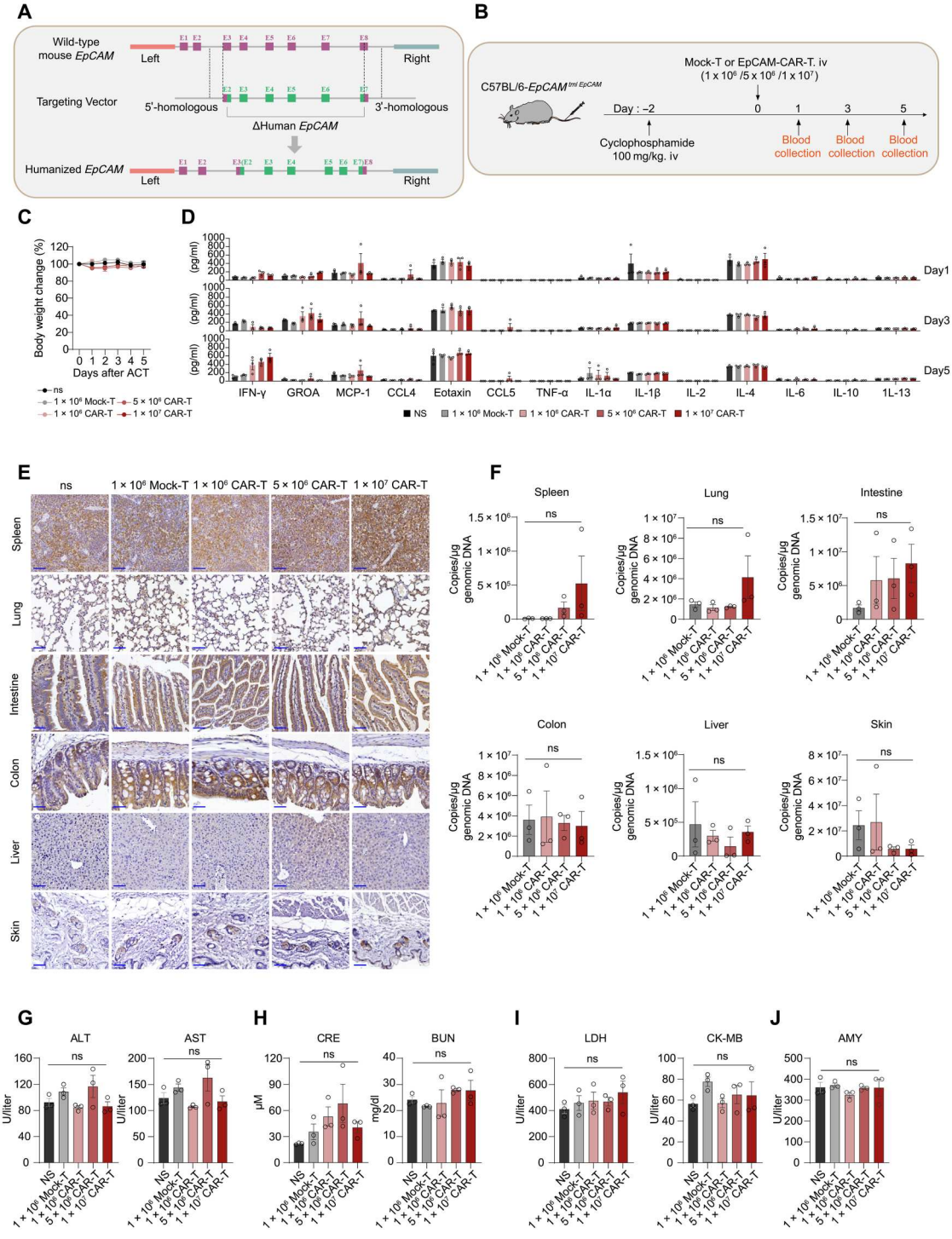

Fig. 3. EpCAM–CAR-T cells were well tolerated by EpCAM-humanized mice. (**A**) Genetic engineering strategy for *EpCAM*-humanized C57BL/6 mice. The murine *EpCAM* gene locus was truncated, and a homologous human *EpCAM* gene locus was inserted from exon 2 to exon 7. Purple, exon of mouse *EpCAM*; green, exon of human *EpCAM*; E, exon. (**B**) Experimental schematic showing the safety evaluation in the C57BL/6-*EpCAM*$^{tml\ EpCAM}$ mouse model. The mice were randomly grouped; $n = 3$ per group. All mice were preconditioned with cyclophosphamide (100 mg/kg). Two days later, a single dose of Mock-T cells (1×10^6) or EpCAM–CAR-T cells (1×10^6, 5×10^6, and 1×10^7) was intravenously administered. (**C**) Percentage of body weight change was normalized to that on day 0 after T cell infusion. (**D**) Serum cytokine levels in peripheral blood at the indicated points after T cell infusion (means ± SD). (**E** and **F**) Representative immunohistochemical (E) and quantitative real-time PCR (F) analysis of mouse $CD3^+$ cells (E) and EpCAM-CAR gene (F) distribution in the spleen, lung, and other organs 7 days after T cell transfer. Scale bars, 50 μm. (**G** to **J**) Organ damage-related serum biomarkers were measured in the liver (G), kidney (H), heart (I), and pancreas (J) on day 7 after T cell transfer. The data are presented as the means ± SD, and data analysis was performed by one-way analysis of variance (ANOVA). $P < 0.05$ was considered statistically significant. AST, aspartate aminotransferase; ALT, alanine aminotransferase; CRE, creatinine; BUN, blood urea nitrogen; LDH, lactate dehydrogenase; CK-MB, creatine kinase-MB; AMY, amylase.

humans. However, these results need to be further confirmed in clinical trials.

Clinical trial design and patient characteristics

Considering the widespread expression of EpCAM in gastric cancer, colon cancer, and other solid tumors (*10*) and the excellent antitumor activity and safety of EpCAM–CAR-T cells in preclinical research (*18*, *35*), we then initiated a phase 1 clinical study of Dectin-1–administrated EpCAM–CAR-T cell therapy with the primary end point of evaluating the safety of the treatment and the secondary end point of evaluating antitumor efficacy (NCT02915445). The Medical Ethics Committee of West China Hospital, Sichuan University approved the study protocol, and all patients provided informed consent.

The clinical design of the study is shown in Fig. 4A. Briefly, patients whose primary or metastatic lesions had high EpCAM expression were enrolled if they met the inclusion criteria. For patients with advanced gastric cancer secondary to peritoneal metastasis, EpCAM–CAR-T cells were intraperitoneally transferred via interventional operation. Patients with colon cancer, rectal carcinoma, and other tumors received intravenous infusion of CAR-T cells. All enrolled patients were treated with preconditional chemotherapy with 300 mg of cyclophosphamide/m^2 plus 30 mg of fludarabine/m^2 before the CAR-T cell infusion. EpCAM–CAR-T cells were administered once they met the release criteria of CAR-T cells, and the patients were treated with a dose escalation design, as shown in Fig. 4A. Then, the adverse effects of the therapy were monitored. Computerized tomography (CT) imaging, inflammatory cytokine detection, and pharmaceutical kinetics analysis by measuring the specific genes of CAR-T cells were performed during the next 6 months. Long-term follow-up of the patients was performed

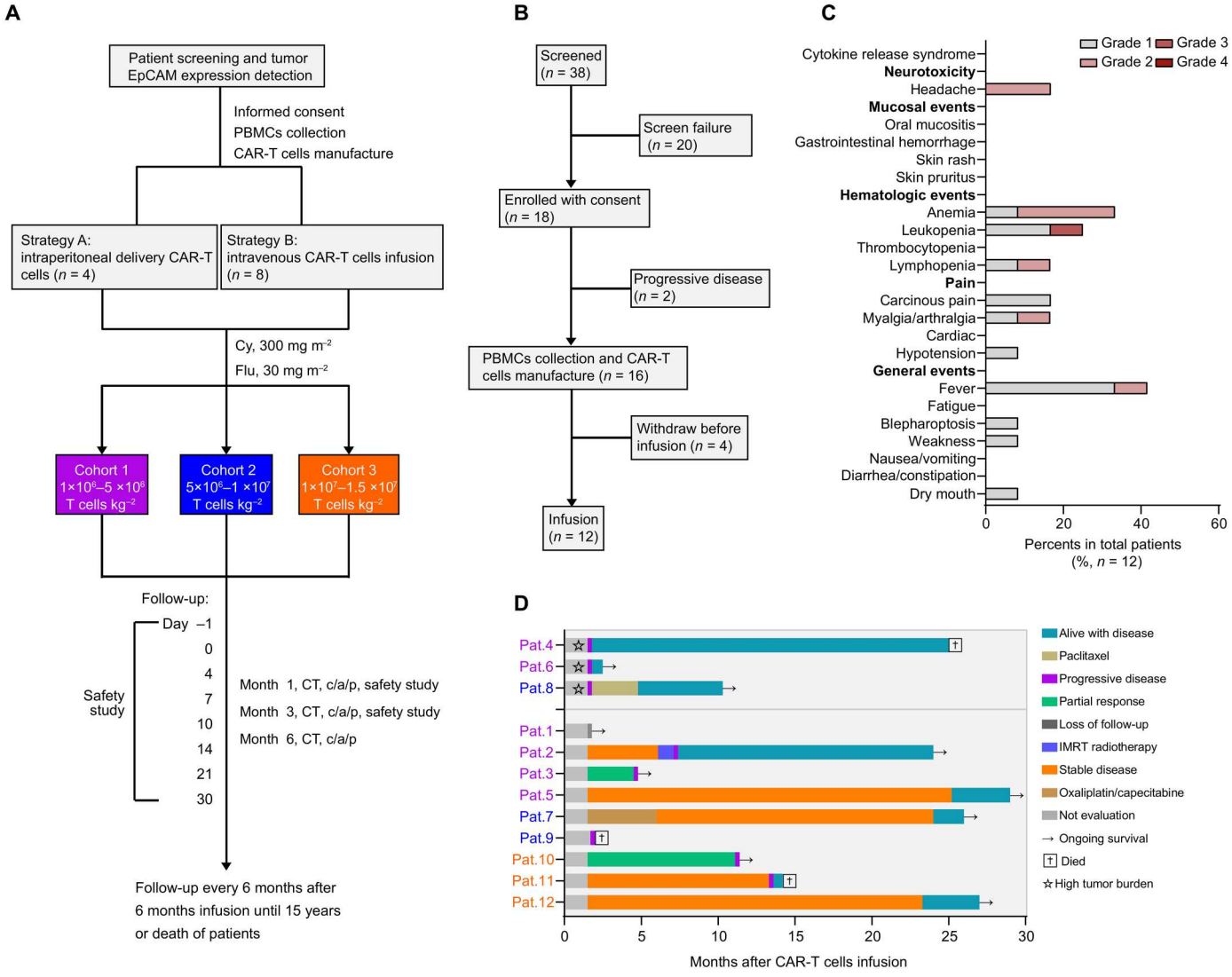

Fig. 4. EpCAM–CAR-T cell clinical protocol design and cohort diagram. (**A**) Clinical protocol schematic for patient screening, CAR-T cell manufacture, and time points of the clinical study. Cy, cyclophosphamide; Flu, fludarabine; CT c/a/p, computed tomography of chest/abdomen/pelvis. (**B**) Number of patients screened, enrolled, and treated with autologous EpCAM–CAR-T cells in the clinical study. (**C**) Waterfall plot summarizing the adverse effects of CAR-T therapy in the clinical study. (**D**) Swimming plot showing patients' disease development and substantial therapy and present status. IMRT, intensity-modulated radiotherapy.

every 6 months beginning 6 months after the infusion of CAR-T cells and lasted until patient death or 15 years.

In this pilot clinical study, 12 patients were enrolled and received autologous EpCAM–CAR-T cell treatment following the inclusion/exclusion criteria. The clinical and disease characteristics of all patients are listed in Table 1. The median age at the beginning of the study was 54.9 years old (from 27.2 to 69.6 years). All patients had stage III or IV advanced carcinoma, and 10 patients had metastases before treatment. Seven patients underwent radical resection plus chemotherapy, and five patients underwent chemotherapy only. All primary or metastatic tumor lesions were EpCAM positive (fig. S7C).

Manufacture and characteristics of EpCAM–CAR-T cells

CAR-T cells were successfully generated from the 16 patients whose peripheral blood mononuclear cells (PBMCs) were collected for CAR-T cell manufacturing. Four patients withdrew from the infusion due to the infeasibility caused by the development of their disease, and 12 patients completed the EpCAM–CAR-T cell treatment (Fig. 4B). Of these 12 patients, lymphocytes were obtained by apheresis ($n = 4$) or peripheral blood collection ($n = 8$). The period time from lymphocyte separation to final product harvest was 11 to 14 days, and the median time was 12 days. EpCAM–CAR-T cells were harvested once they met the release criteria of CAR-T cells. The final CAR-T cell products were immediately infused or cryopreserved.

After the CAR-T cells were harvested, we analyzed the final cell products by flow cytometry. In all infused cell products, most were T cells. The median percentage of $CD3^+$ cells was 97.88% (range, 77.37 to 99.94%). $CD3^+$ T lymphocytes contained a mixture of $CD4^+$, $CD8^+$, and $CD56^+$ subpopulation cells with patient-specific heterogeneity and wide-ranging subset distributions. The median frequency of $CD4^+$ helper T cells was 44.81%, ranging from 15.42 to 91.48%. The proportion of $CD8^+$ T lymphocytes ranged from 6.93 to 77.95% (median frequency, 48.64%). A small group of cells were identified as $CD56^+$ cells (median, 14.59%; range, 3.57 to 19.25%). The median CD4:CD8 T cell ratio in the infused products was 1 (range, 0.2 to 13.2). In addition, the CAR^+ cell frequency in the final patient-infused products is 22.07%, ranging from 5.03 to 90.68%. These data demonstrated our stable and efficient EpCAM–CAR-T cell manufacturing capability.

Safety evaluation of autologous EpCAM–CAR-T cells in patients with EpCAM-expressing carcinomas

For this clinical study, the primary end point was the safety of EpCAM–CAR-T therapy. The adverse events were categorized according to the Common Terminology Criteria for Adverse Events Version 5.0 (CTCAE 5.0) and are listed in table S1 and summarized in Fig. 4C. In cohort 1, six patients received a single dose of 1×10^6 to 5×10^6/kg T cells by infusion. Four subjects experienced grade 1/2 acute fever, myalgia or arthralgia pain, dry mouth, blepharoptosis, hypotension, leukopenia, and weakness after autologous EpCAM–CAR-T cell transfer (patients 1, 3, 5, and 6). Two of these patients developed concurrence metastasis lesion-limited pain within 1 month. One patient underwent progression of leukopenia from grade 1 before infusion to grade 3 after treatment, which resolved after drug intervention (patient 3). Moreover, there was no evidence of neurological toxicity except for two recipients who had suffered from grade 2 headache (patient 1 and patient 6). All adverse events in the cohort 1 group were mild and self-remitted without any intervention except for grade 3 leukopenia. In cohort 2, three subjects received one dose of 5×10^6 to 1×10^7/kg T cells by infusion. Only one patient developed grade 1 lymphopenia, and another suffered from grade 1 acute fever within 1 week of treatment. In cohort 3, only one patient developed grade 1 acute fever without any other adverse events. Among all patients, no CRS evidence was observed, and five tolerated EpCAM–CAR-T therapy without any detectable therapy-associated toxicity. No skin events, gastrointestinal hemorrhage, oral mucositis, or other EpCAM-directed grade ≥3 toxicities or dose-limiting toxicities were identified in any patient. Moreover, no subject died from this therapy.

EpCAM–CAR-T cell persistence and cytokine release after transfusion

We analyzed EpCAM–CAR-T cell persistence and cytokine kinetics in many subjects after infusion. As shown in Fig. 5A, there was measurable persistence of CAR-T cells without obvious CAR-T cell expansion within 1 month of treatment in the groups. In cohort 2 and cohort 3, although there was no evidence of large CAR-T cell expansion in a short time, we observed high levels of serum CAR-T cell persistence 200 days after infusion in two patients (patient 7 and patient 10). Patient 10 reached the peak CAR-T cell number on day 7, which declined to the measurable baseline in subsequent monitoring. For cytokine kinetics, there was a mild increase in IL-6 and tumor necrosis factor–α (TNF-α) in all subjects (Fig. 5, B and C). Most patient serum IL-6 reached the peak concentration on day 3 and TNF-α on days 14 to 22 after infusion, and the change in serum complement-reactive protein (CRP) was not obvious (Fig. 5D). These results suggested that EpCAM–CAR-T cell infusion did not markedly increase cytokines, which correlated with a low risk of CRS in this therapy.

Antitumor effects of EpCAM–CAR-T cells

The clinical response was assessed on the basis of Response Evaluation Criteria in Solid Tumors 1.1 (RECIST 1.1). Preliminary antitumor efficacy was evaluated by CT and is summarized in Fig. 4D. After images were compared pre– and post–CAR-T cell administration in all enrolled patients, five patients remained with a stable disease after CAR-T cell administration. Among these patients, three achieved progression-free survival longer than 700 days. Of the other enrolled patients, eight experienced progressive disease, and one patient was lost to follow-up 2 months after T cell infusion. Evidence of tumor regression was observed in patient 10 and patient 3 (Fig. 5E). In cohort 3, patient 10 received one high dose of T cell infusion via the peritoneum, and the tumor in the peritoneum was remitted after 7 months of treatment (Fig. 5E). This finding was consistent with the high CAR gene copies in peripheral blood on day 200 (Fig. 5A), suggesting that CAR-T cells had long-term persistence in patient 10. In cohort 1, patient 3 achieved a partial response in lung tumors 3 months after treatment (Figs. 4D and Fig. 5E) but subsequently developed disease progression due to increased lung metastasis. This may be attributed to the intravenous infusion strategy and low dose of infused CAR-T cells, which resulted in short-term CAR-T cell persistence in vivo (Fig. 5A).

In addition, the clinical response was associated with tumor burden. Patients whose original tumor lesions were removed were more likely to maintain stable disease and achieve longer progression-free survival. High tumor burden and multiple metastases

Table 1. Clinical characteristics of enrolled patients. 5-FU, fluorouracil; B-II, Billroth II; BV, bevacizumab; CF, calcium folinate; Cis, cisplatin; CP, cyclophosphamide; dFdC, gemcitabine; HIPEC, hyperthermic intraperitoneal chemotherapy; Ifos, ifosfamide; IRT, irinotecan; L-OHP, oxaliplatin; LND, lymph node dissection; LRRCC, laparoscopic radical resection of rectal carcinoma; mFOLFOX6, oxaliplatin + calcium folinate + fluorouracil; MRND, modified radical lymph node dissection; PTX, paclitaxel; R, radical resection; RFA, radiofrequency ablation; RLG, radical laparoscopic distal gastrectomy; RPN, resection of pulmonary nodules; RSCC, radical resection of sigmoid colon cancer; S-1, tegafur gimeracil oteracil; XELOX, capecitabine plus oxaliplatin; Y, yes; N, no.

Cohort	Patient no.	Gender	Age (years)	ECOG score	Diagnosis disease	Disease location	Previous treatment				T cell dose (cells/kg)	CAR^+ (%)
							Surgery	Chemotherapy	Radiation therapy	Other agents		
1	1	Male	44.6	1	Nasopharynx cancer, IIIC	Nasopharynx, liver, lung, bone	Neck MRND	Cis. Cis, Tegafur × 2. Ifos, Vinorelbine	Y	Docetaxel, dFdC	$1.64 \times 10^{+06}$	42.99
	2	Male	46.7	1	Nasopharynx cancer, IIIB	Nasopharynx, lung	N	Cis, CP. Cis	Y	Docetaxel, dFdC	$1.78 \times 10^{+06}$	5.03
	3	Male	47.6	1	Parotid gland cancer, IVA	Lung	N	Cis. Cis, tegafur (2×)	Y	dFdC	$3.92 \times 10^{+06}$	12
	4	Female	58.3	1	Colon cancer, IVA	Lung, pelvic cavity	LRRCC, RPN	L-OHP, S-1. IRT, CF, 5-FU. mFOLFOX6	Y	BV, anlotinib	$2.64 \times 10^{+06}$	91.50
	5	Female	68.7	0	Rectal carcinoma, IIIB	Pelvic cavity, abdominal wall	LRRCC	L-OHP, CF, 5-FU (12×)	Y	N	$2.78 \times 10^{+06}$	31.94
	6	Male	50.9	1	Nasopharynx cancer, IIIC	Nasopharynx, liver, bone	R	dFdC, vinorelbine	Y	N	$3.35 \times 10^{+06}$	10.14
2	7	Male	69.6	0	Gastric cancer, IV	Omentulum	RLG, D2 LND, B-II	Intraperitoneal PTX, XELOX. HIPEC	N	N	$7.69 \times 10^{+06}$	7.52
	8	Male	67.2	1	Gastric cancer, IV	Peritoneum	N	Intraperitoneal PTX, XELOX. HIPEC	N	N	$9.52 \times 10^{+06}$	90.68
	9	Female	51.5	1	Gastric cancer, IV	Stomach	N	Intraperitoneal PTX, XELOX. HIPEC	N	N	$9.79 \times 10^{+06}$	18.55
3	10	Male	69.4	1	Gastric cancer, IV	Stomach	N	HIPEC (3×)	N	N	$1.58 \times 10^{+07}$	25.59
	11	Female	27.2	1	Signet-ring cell carcinoma, IV	Colon sigmoideum, liver	RSCC	mFOLFOX6 (2×), L-OHP	Y	N	$1.63 \times 10^{+07}$	50.57
	12	Male	64.6	0	Rectal carcinoma, IIIC	Pelvic cavity, abdominal wall	LRRCC	XELOX	N	N	$3.52 \times 10^{+07}$	9.30

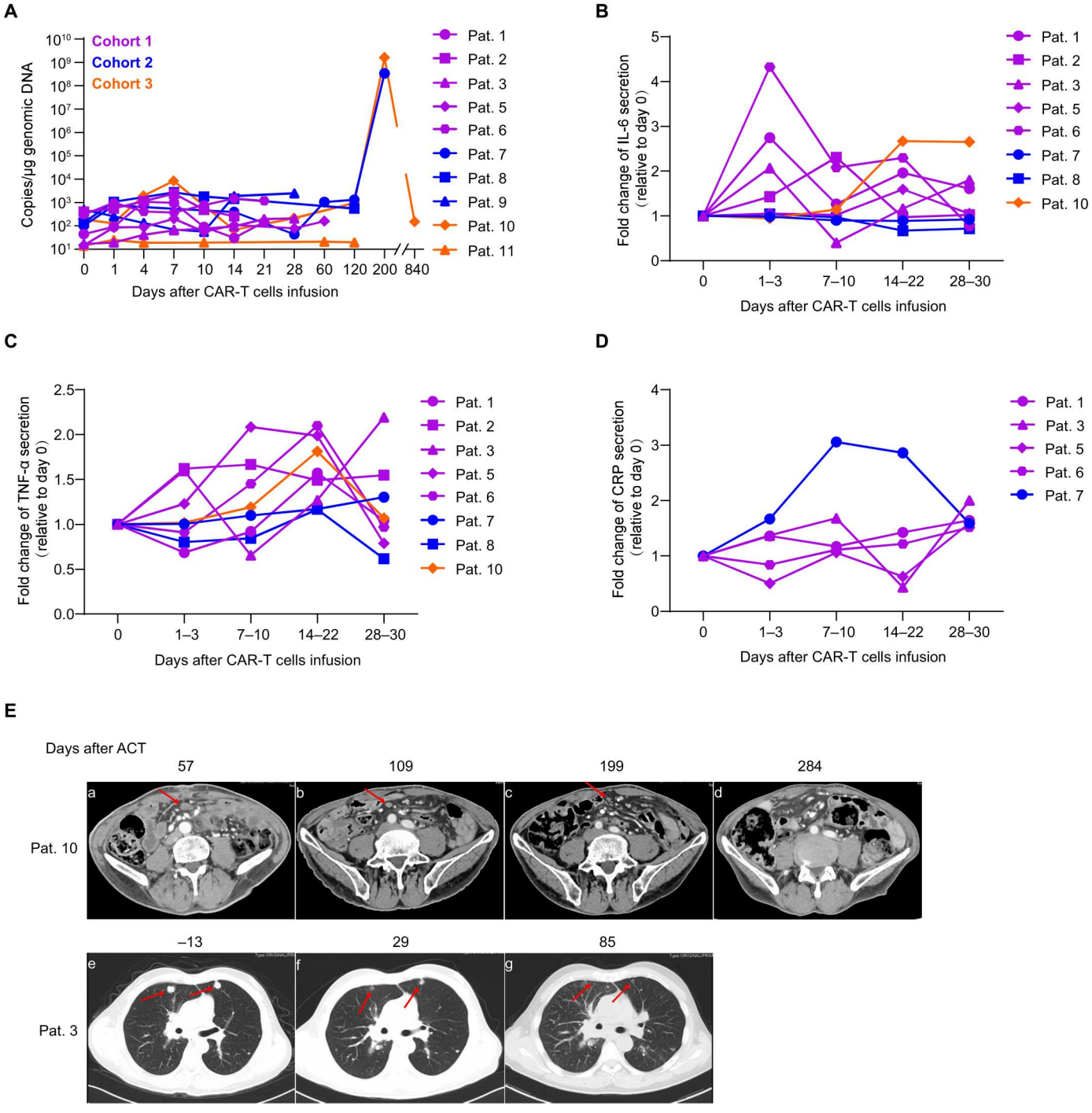

Fig. 5. EpCAM–CAR-T cell persistence, cytokine secretion and radiologic evaluation of patients after EpCAM–CAR-T cell infusion. (**A**) EpCAM-CAR gene copies in genomic DNA of peripheral blood from patients at the indicated times following CAR-T cell transfer. (**B** to **D**) Representative serum IL-6 (B), TNF-α (C), and CRP (D) levels in patients treated with EpCAM–CAR-T cells. Cohort 1: violet; cohort 2: blue; cohort 3: orange. (**E**) Computed tomography scans showing the tumor response in patient 10 and patient 3 after EpCAM–CAR-T cell transfer. Red arrows indicate the tumor site.

before infusion predicted poor prognosis (Fig. 4D and Table 1). Although CAR-T cells have measurable proliferation and mild cytokine secretion after infusion (Fig. 5, A to D), there was no treatment-related CRS in any of the patients as evaluated by former reported CRS diagnosis criteria (*36*). Long-lasting antitumor efficacy in surviving patients is still being monitored.

DISCUSSION

CAR-T cell–based cancer immunotherapy has shown therapeutic potential for the treatment of hematological malignancies, and endeavours have been made to extend this efficacy to solid tumors. To solve many barriers that cause poor responses of solid tumors to CAR-T therapy, optimization of the clinical strategy and updating CAR architecture remain the key factors to success for this novel therapy. Careful demonstration of the feasibility of the tumor antigen targeted by CAR-T cells, efficient intracellular signaling, and the delivery pathway of CAR-T cells are the focuses of researchers worldwide (*37*). As a surface molecule that is overexpressed on tumor cells, EpCAM has been deemed an attractive target for cancer therapies. Various strategies targeting EpCAM molecules have demonstrated therapeutic potential in previous investigations (*16*, *17*, *38*); however, the clinical feasibility of CAR-T therapy targeting EpCAM is lacking. In this study, we designed a specific EpCAM-directed CAR construct bearing a Dectin-1 intracellular costimulatory domain and demonstrated the safety and efficacy of EpCAM–CAR-T cell therapy in preclinical and clinical studies.

First, the specific cytotoxicity of the EpCAM–CAR-T cells was examined (fig. S1), and it was dependent on the density of the antigen on the tumor cells (fig. S4). Several studies have demonstrated that the therapeutic benefit of CAR-T cells might ultimately be dependent on optimal intracellular signaling transduced by the costimulatory molecules (*20*, *39*). In this study, we selected the intracellular domain of Dectin-1 (*CLEC7A*, C-type lectin domain family 7 member A), which is a new peptide sequence, as the costimulatory domain in the CAR construct. In a preliminary study of this CAR construct, our team demonstrated that HER2-specific CAR-T cells bearing the Dectin-1 costimulatory domain exhibited different phenotypes and biological functions from those of CD28 CAR-T cells (*40*). Although detailed mechanism by which Decint-1 intracellular domain exerts the biological functions in CAR-T cells is unclear, several clues facilitate the elucidation of the advantage of the Dectin-1 CAR-T cells. In this study, it is found that after being exposed to the antigen, Dectin-1 CAR-T cells were prone to develop more central memory T cell phenotype compared with the classic CD28 costimulatory domain–engaged CAR-T cells and less terminal effector T cell phenotype compared with 4-1BB CAR-T cells in vitro and in vivo (Fig. 1 and fig. S1). These findings suggested that Dectin-1–stimulated EpCAM–CAR-T cells have appropriate persistence and sustained therapeutic efficacy (*41*), which has been further validated in xenograft models. The satisfactory therapeutic effects, good infiltration, and long-lasting survival of Dectin-1 bearing EpCAM–CAR-T cells in xenograft models were observed (Figs. 1 and 2). In addition to the central memory phenotype, reduced self-activation and exhaustion might contribute to the functionality of Dectin-1 CAR-T cells in vivo. A previous study reported that the signaling activation strength of CAR-T cells is a key determinant for the sustained activity of CAR-T cells (*42*). In this study, we observed that Dectin-1 CAR-T cells showed moderate activation levels of immune function of T cells (Fig. 1). *NR4A1* has been identified as a key mediator of T cell hyporesponsiveness and limits CAR-T cell function in solid tumors (*27*, *43*). Also, *c-Jun* deficiency mediates CAR-T cell dysfunction, and engineering CAR-T cells to overexpress *c-Jun* endows CAR-T cells with exhaustion resistance (*29*). In this study, we found that decreased *NR4A1* and increased of *JUN* expression (fig. S1), as well as diminished expression of immune checkpoint receptors PD-1 and LAG-3 in Dectin-1 CAR-T cells, indicate decreased exhaustion tendency of Dectin-1–costimulated CAR-T cells. However, to fully understand the properties of this specific CAR construct and clarify the mechanism, additional experiments, especially further in vivo experiments of Dectin-1 CAR-T cells, are needed. Considering these advantages of Dectin-1 CAR-T cells in self-activation, exhaustion, and rigorous tumor killing ability, we lastly selected the Dectin-1 intracellular domain as the costimulatory effector for this second generation of EpCAM-specific CAR-T cells.

Two delivery pathways of EpCAM–CAR-T cells were used to confirm the antitumor efficacy and safety in animal models. As shown in Fig. 2, both intravenous and intraperitoneal infusion of EpCAM–CAR-T cells robustly inhibited tumor growth. Compared with intravenous infusion, intraperitoneal infusion of CAR-T cells requires a lower number of CAR-T cells to control the growth of tumors. This difference might be due to the efficient trafficking of CAR-T cells into the tumor mass via the local delivery pathway. A preclinical result demonstrated that, compared with systemically infused CAR-T cells, 30-fold fewer dose of intrapleurally administered CAR-T cells can induce long-term complete remission for malignant pleural mesothelioma treatment. Even equivalent numbers of CAR-T cells accumulated in pleural tumor, systemically infused CAR-T cells cannot achieve persistence and eradicate tumor (*9*). In addition, there is no obvious difference in safety for these two CAR-T cell delivery strategies in the corresponding clinical research (*44*). Also, the therapeutic potential of local delivery pathways, such as intertumoral injection (*45*) and intracranial injection (*46*, *47*), has been validated in previous studies. Notably, intraventricular administrated IL-13Rα2 CAR-T cells displayed curative efficacy for patient with recurrent multifocal glioblastoma (*47*), suggesting the therapeutic potential of locally delivered CAR-T cells for specified tumors. In our clinical study, four gastric cancer patients received locally delivered EpCAM–CAR-T cells and patient 10 has a partial response (Fig. 4E) and patient 7 has a >2-year survival. Because of the limited number of enrolled patients, to confirm the clinical benefit of locally infused CAR-T cells, more trials, such as intracranial infusion of CAR-T cells (*47*), and clinical data for comprehensive elucidation of the advantages are needed.

Our preclinical research initially focused on the safety and efficacy of EpCAM–CAR-T cell therapy, and so we designed and generated an EpCAM-humanized immunocompetent mouse model to evaluate the potential off-target toxicity of EpCAM-CAR-engineered T cells. We observed human EpCAM expression in the alimentary canal, nephric tubule, skin, and pulmonary alveoli of humanized mice, which was consistent with the expression pattern of EpCAM in humans. This transgenic mouse model served as an in vivo platform that could mimic the expression pattern of human EpCAM in mice, which is, at least in part, different from that of mouse EpCAM. To determine the cytotoxicity of EpCAM–CAR-T cells, different doses (1×10^6, 5×10^6, and 1×10^7 cells) of EpCAM–CAR-T cells were infused into EpCAM-

humanized immunocompetent mice. After EpCAM–CAR-T cell administration, no dose-dependent toxicity was observed (Fig. 3). No obvious evidence that T cell infiltration and tissue damage occurred in tissues after CAR-T cell infusion. Qin *et al.* (*48*) found that EpCAM–CAR-T cells were harmless to normal tissues except the lung. Although our humanized mice exhibited obvious EpCAM expression on alveolar cells and bronchial cells, we did not detect any lung injury in response to EpCAM–CAR-T cells. These results may be explained by the different affinities of the recognition domains of the CAR-T cells and different CAR-T cell infusion doses. Morgan *et al.* (*5*) showed that high-dose HER2-specific CAR-T cells induced inflammatory cytokine secretion and lethal toxicity due to the low expression of HER2 antigen on lung epithelial cells. However, similar toxicity has not been observed in lower-dose HER2–CAR-T cell treatment (*49*), suggesting that a customized treatment dose is necessary for patients. The high affinity of the antigen-recognition domain should be responsible for antigen-induced fatal toxicity (*50*, *51*). The ability to recognize antigens is dependent on the affinity of scFv, while hyperactivation caused by excessive affinity can trigger T cell depletion and other toxicity (*52*, *53*). Therefore, finding the balance between affinity and function may improve treatment safety by ensuring the efficiency of recognition (*4*). Therefore, the safety of targeted cellular therapy is affected by numerous factors, including therapeutic dose, target toxicity, affinity of the recognized domain, and tonic signaling. Combined with the absence of cytotoxicity to normal tissues in immunodeficient mice and EpCAM-humanized mice and a previous study in which we found that third-generation EpCAM–CAR-T cells induced good tumor regression in a xenograft model without obvious treatment-related cytotoxicity (*35*), we moved EpCAM–CAR-T cells bearing the Dectin-1 costimulatory domain into a clinical trial.

The primary end point was to evaluate safety, and the secondary goal was to evaluate efficacy. We initiated that pilot phase 1 clinical trials use EpCAM–CAR-T cells to treat tumors. In this study, EpCAM–CAR-T cells were infused in a dose-escalating manner. Three cohorts received 1×10^6 to 5×10^6, 5×10^6 to 10×10^6, or 10×10^6 to 15×10^6 cells/kg EpCAM–CAR-T cells. There were no severe adverse effects detected in any cohort, except patient 3, who underwent grade 3 leukopenia, to which lymphodepletion and previous chemotherapy were mainly ascribed. CRS and neurotoxicity were not observed in any of the subjects. Last, the most tolerable dose was not reached.

The robust release of inflammatory cytokines and the proliferation of CAR-T cells contribute to antitumor efficacy in the treatment of hematological malignancies (*54*). In this study, we performed lymphodepletion by preconditional chemotherapy and CAR-T cell proliferation and increased cytokines in peripheral blood after 1 month of treatment were detected (Fig. 5), but the expansion fold and cytokines levels were much lower than that in CAR-T therapy in treatment of hematological malignancies. This may be attributed to the different kinetics of CAR-T cells in solid tumors and hematological malignancies (*36*, *55*). In two patients (patient 7 and patient 10) in cohorts 2 and 3, infused CAR-T cells were detected at high levels 200 days after infusion. Although previous clinical instances highlight the probability of CAR-T cells malignant transformation (*56*, *57*), we had not detected such transformation and CRS evidence in patient 7 and patient 10. Long-term persistence of CAR-T cells in patient 10 contributed, at least in part, to the antitumor efficacy for this subject, whose partial response lasted 10 months. In the treatment of solid tumors, CAR-T cell homing to tumor lesions limited CAR-T cell persistence in peripheral blood, especially locally infused CAR-T cells (*47*). Although long-term persistence of EpCAM–CAR-T cells was found in two subjects, further investigations and more clinical cases are needed to determine the correlation between peripheral CAR-T cell levels and the clinical benefits to solid tumors.

In this study, the absence of robust cytokine release—especially IL-6, TNF-α, and CRP—might be related to the safety of EpCAM–CAR-T cell therapy. Although inflammatory cytokines increased after the infusion of CAR-T cells, especially in subjects in the high-dose cohorts, the levels of cytokines in most of the patients returned to baseline (Fig. 5). In patient 10, IL-6 and TNF-α were released at high levels after infusion. This effect might be closely related to the long-term persistence of EpCAM–CAR-T cells. Many factors affect cytokine release by CAR-T cells in solid tumors. The harsh microenvironment in solid tumors inhibits the function of CAR-T cells, including the persistence, proliferation, infiltration, and release of inflammatory cytokines. In addition, in this study, the EpCAM antigen was targeted by CAR-T cells, and whether the characteristics of the antigen affect cytokine release and other properties of EpCAM–CAR-T cells remains unclear.

In summary, we designed a specific CAR construct with EpCAM specificity and examined the antitumor potential of EpCAM–CAR-T cells in preclinical and clinical investigations. Moreover, the safety of EpCAM–CAR-T cells was verified in an *EpCAM*-humanized mouse model and immunodeficient mice. To further evaluate the feasibility of EpCAM–CAR-T therapy, a clinical investigation of autologous EpCAM–CAR-T cell therapy for solid tumors demonstrated its safety and efficacy. Further properties of the EpCAM–CAR-T cells and the mechanisms contributing to the clinical benefits of this therapy require larger-scale clinical investigations.

MATERIALS AND METHODS

Cell lines and culture conditions

The Lentivirus package human embryonic kidney (HEK) 293T (HEK-293T) cells were purchased from the American Type Culture Collection (Manassas, VA). Human cancer cell lines—including the ovarian cancer cell line SK-OV-3, lung adenocarcinoma cell line A549, breast cancer cell line MDA-MB-468, cervical carcinoma cell line HeLa, and colorectal adenocarcinoma cell line HT-29—were obtained from the Chinese Academy of Sciences. HeLa cells were transduced with lentiviruses encoding human EpCAM. After being screened by puromycin, resistant monoclonal cells were selected. HeLa cells expressing EpCAM were identified by flow cytometry after being stained with anti-human EpCAM antibodies. The fluorescent reporter gene *Luc* was introduced into HT-29 cells (HT-29–Luc) by lentiviruses. The puromycin-resistant HT-29–Luc cells were identified by an In Vivo Imaging System (IVIS). HEK-293T, SK-OV-3, HT-29, and HeLa cells were cultured in Dulbecco's modified Eagle's medium (Gibco) containing 10% (v/v) bovine serum (PAN), penicillin (100 U/ml), and streptomycin (100 mg/ml; HyClone). A549 cells were cultured in RPMI 1640 medium (Gibco) supplemented with 10% (v/v) bovine serum (PAN), penicillin (100 U/ml), and streptomycin (100 mg/ml; HyClone). The cells were cultured in a humidified incubator at 37°C supplemented with 5% CO_2.

Mice

Female B-NDG mice were purchased from Biocytogen Inc. (6 to 8 weeks old). The generation of genetically modified mice (C57BL/6-*EpCAM*$^{tml\ EpCAM}$) was entrusted to Biocytogen Inc. All animals were fed and bred under specific pathogen–free conditions in the Laboratory Animal Center of State Key Laboratory of Biotherapy. All animal experiments were conducted according to the animal health care regulations of the ethics committee in the State Key Laboratory of Biotherapy, Sichuan University.

Structural design of the CAR

The EpCAM-CAR was constructed and optimized on the basis of the second-generation CAR construct. Briefly, the CAR was composed of a signal peptide from human IL-2; a human EpCAM-specific nanobody (VHH); a CD8α hinge; a transmembrane and an intracellular domain derived from Dectin-1, CD28, or 4-1BB; and an immunoreceptor tyrosine-based activation motif 1 (ITAM1) domain derived from human CD3ζ.

Multiple anti-human HER2-specific CARs were designed on the basis of the second-generation CAR construct. They all consisted of human CD8α signal peptide and hinge domain, human HER2-specific scFv derived from the FRP5 monoclonal antibody, and the CD3ζ signal in the C-terminal. Moreover, these constructs had the characteristics of different intracellular costimulatory domains and transmembrane regions, which were derived from CD28, 4-1BB, or Dectin-1. All DNA coding CAR molecules were cloned into the lentiviral vector pCLK.

Package and purification of lentivirus

Three plasmid systems and the calcium phosphate method were used to produce the lentivirus by transfecting the packaging plasmids psPAX2 and pMD2. G (Invitrogen) and the transgene expression plasmid pCLK into HEK-293T cells. Mock lentivirus was generated using package plasmids and a non-CAR–expressing pCLK backbone. Supernatants containing the lentiviral particles were harvested 48 and 72 hours after transfection, followed by concentration and purification by filtration and ultracentrifugation at 19,700 rpm/min (BECKMAN). Last, the viral titter of the purified product was determined by quantitative real-time polymerase chain reaction (PCR).

Transduction of human T cells

Human PBMCs from healthy donors were isolated with Ficoll-Paque (Sigma-Aldrich). Primary $CD3^+$ T cells were enriched from human PBMCs using the CD3 Fab-TACS Agarose Column Starter Kit (IBA Lifesciences). The isolated $CD3^+$ T cells were stimulated with anti-CD3/anti-CD28 Dynabeads (Gibco) and cultured in X-VIVO 15 medium (Lonza) supplemented with recombinant human IL-2 (hIL-2) (100 IU/ml; PeproTech), hIL-7/IL-15 (10 μg/ml; Novoprotein), and 5% (v/v) human serum (Sigma-Aldrich). After 24 hours, the prestimulated T cells were transduced with lentivirus containing the different CAR fragments. During this experiment, FibroNectin (Tonglihaiyuan Biotech)–coated plates were used to promote infection. After transduction, human CAR-T cells were expanded for subsequent analysis and provided fresh medium periodically.

Generation of murine CAR-T cells

Fresh murine lymphocytes were isolated from the lymph nodes of mice. Primary mouse lymphocytes were added to a six-well plate that was precoated with anti-mouse CD3 and CD28 antibodies (BioLegend) for T cell activation. The isolated T cells were maintained in RPMI 1640 (Gibco) supplemented with 10% fetal bovine serum (Gibco), mouse IL-2 (100 IU/ml; PeproTech), penicillin (100 U/ml), streptomycin (100 mg/ml; HyClone), 2 mM L-glutamine (Gibco), 1 mM sodium pyruvate (Gibco), 0.1 mM nonessential amino acids (Gibco), and 0.05 mM β-mercaptoethanol (Sigma-Aldrich). After 48 hours, the preactivated T cells were transduced with lentivirus in the presence of polybrene (8 μg/ml). CAR expression on murine T cells was detected by flow cytometry.

CAR-T cell manufacture for clinical usage

The EpCAM–CAR-T cells for clinical use were manufactured from PBMCs isolated by Ficoll-Paque (Sigma-Aldrich). After 24 hours of prestimulation with anti-CD3/anti-CD28 Dynabeads (Gibco), $CD3^+$ T cells were transduced with lentivirus containing the EpCAM-CAR gene and expanded for 11 to 14 days. Rigorous quality control was performed during therapeutic CAR-T cell preparation. All procedures on EpCAM–CAR-T cells were carried out under good manufacturing practice (GMP) conditions.

Flow cytometry

For surface CAR expression assessment, engineered T cells were incubated with Alexa Fluor 488–conjugated anti-camel VHH antibodies (clone: 96A3F5, GenScript) or HER2-Fc protein (Novoprotein) at 4°C for 45 min. Then, the HER2–CAR-T cells were reacted with fluorescein isothiocyanate–labeled anti-Fc antibodies (Sigma-Aldrich, catalog no. F9512) and analyzed by flow cytometry. 7-Aminoactinomycin D (7-AAD) (BioLegend) staining was performed to discriminate dead cells from total cells. For extracellular staining, the cells were washed and resuspended in phosphate-buffered saline (PBS) buffer. Fluorochrome-conjugated antibodies were incubated with the cells at 4°C for 30 min in the dark. Flow cytometry was performed on a NovoCyte flow cytometer (ACEA) and analyzed by NovoExpress 1.3.0 software (ACEA).

Antibodies

The immunophenotyping of T cells was performed with various monoclonal antibodies, including anti-CD3 (clone: HIT3A, BioLegend), anti-CD4 (clone: RPA-T4, BioLegend), anti-CD8 (clone: HIT8A, BioLegend), anti-CD45RA (clone: HI30, BioLegend), anti-CD62L (clone: preg-56, BD), anti–PD-1 (clone: NA7105, BioLegend), anti-TIM-3 (clone: F38-2F2, BioLegend), anti–LAG-3 (clone: 7H2C65, BioLegend), anti-CD25 (clone: O323, BioLegend), anti-CD27 (clone: O323, BioLegend), anti-CD28 (clone: CD28.2, BioLegend), anti-CD69 (clone: FN50, BioLegend), anti-CD127 (clone: A01905, BioLegend).

Granzyme B secretion was tested using an anti-human Granzyme B recombinant antibody (clone: QA16A02, BioLegend). Monoclonal anti-human EpCAM antibodies (clone: 9C4, BioLegend) and anti-human HER2 antibodies (clone: 4D5, BioLegend) were used to detect EpCAM or HER2 expression on the tumor cell surface.

To detect CAR-T cells in vivo, peripheral heparinized blood or primary spleen cell suspensions were pretreated with Red Blood Cell Lysis Buffer (Solaria) and stained with anti-camel VHH antibodies

(clone: 96A3F5, GenScript) and anti-hCD45 antibodies (clone: HI30, BioLegend).

Clinical trial

This clinical trial was a phase 1, multicentre and open-label study that was initiated to investigate the safety and efficacy of EpCAM–CAR-T cells in patients with primary and relapsed stage III or IV advanced solid tumors. The study protocol was reviewed and approved by the Medical Ethics Committee of West China Hospital of Sichuan University. This clinical study was registered at ClinicalTrials.gov with the identifiers NCT02915445. After explaining the potential risks, written informed consent was obtained from the patients. Then, autologous EpCAM–CAR-T cells were transferred to patients by intraperitoneal (gastric cancer patients) or intravenous injection (doses ranging from 1.6×10^6 to 3.5×10^7 cells/kg body weight). All therapeutic EpCAM–CAR-T cell products were processed under GMP conditions. Therapy-related adverse events were evaluated during the phase 1 clinical trial according to CTCAE 5.0. Clinical responses were recorded and analyzed on the basis of RECIST 1.1.

Quantitative detection of cytokines

Genetically engineered T cells (CAR-T or Mock-T) were cocultured with tumor cells (1×10^4 antigen-positive or negative cells per well) in 96-well plates at different effector to target (E/T) ratios. After 24 hours, the culture supernatant was collected, and cytokine levels were measured. The production of cytokines, including IFN-γ, TNF-α, and IL-2, was quantified by an ELISA MAX Deluxe Set Human (BioLegend). To simultaneously detect multiple murine serum cytokines, samples were collected and analyzed by using a Luminex Mouse Discovery Assay (R&D Systems).

EpCAM–CAR-T cells were incubated with HeLa cells or EpCAM-expressing HeLa cells (H^{Low}, H^{Mid}, and H^{High}) at 2.5:1 E/T ratio, then brefeldin A was added after 1 hour of coculture. All cells were collected and washed with phosphate buffer after 4 hours of coculture. Next, samples were stained with Alexa Fluor 488–anti camel VHH antibody and fixed with fluorescence-activated cell sorting buffer for 10 min in 4°C. A 0.04% Triton-X 100 was added to permeabilize samples for 10 min in 4°C. Last, cells were stained with allophycocyanin (APC)-anti human Granzyme B antibody for 30 min in 4°C and washed twice for flow analysis.

Real-time cytotoxicity assay

The cytotoxicity of CAR-engineered T cells was monitored and profiled by the xCELLigence Real-Time Cell Analysis System (Agilent). Tumor cells were precultured in E-Plate 96 for 24 hours (1×10^4 per well), followed by the addition of CAR-T cells or Mock-T cells according to the plan. The change in the cell index reflected the target cell attachment and growth characteristics and revealed the cytolytic ability of CAR-T cells. The data were analyzed according to the manufacturer's instructions (RTCA Software 2.1).

Xenograft mouse model

Female B-NDG mice (aged 6 to 8 weeks) were implanted with 2×10^5 HT-29–Luc cells. Seven days later, mice were randomly separated into different groups. Three doses of Mock-T cells or CAR-T cells were adoptively transferred to mice via peritoneum or tail vein on days 0, 3, and 7, respectively. Tumor growth was regularly monitored by BLI. Bioluminescence signals were analyzed on an IVIS Spectrum imaging system (PerkinElmer). During the experiment, mouse body weight and survival were recorded. When all mice were euthanized in the Mock-T–cell treated group, the other mice were subsequently euthanized (above 40 days after CAR-T cells infusion). The orbital blood of mice was collected to determine CAR-T cell persistence in the peripheral blood, the main organs were collected to perform pathological analysis, and tumors were collected simultaneously to detect CAR-T cell infiltration. Many mice were euthanized after 21 days of adoptive T cells treatment. Flow cytometry was used to test the phenotypes and the expression of exhaustion markers in persisted CAR-T cells in vivo.

Safety evaluation mouse model

To test the safety of EpCAM–CAR-T cells with an immunocompetent system, cyclophosphamide (100 mg/kg) was intravenously injected into C57BL/6-*EpCAM*$^{tml\ EpCAM}$ mice (aged 6 to 8 weeks), followed by the adoptive cell transfer of 1×10^6 Mock-T cells, 5×10^6 EpCAM–CAR-T cells, or 1×10^7 EpCAM–CAR-T cells 2 days later. On the first, third, and fifth days after genetically engineered T cells were administered, peripheral heparinized blood samples were collected in each group to evaluate serum cytokine levels. On day 7, all mice were euthanized, and the key organs were isolated and preserved in formalin for further analysis.

For safety evaluation under the tumor-bearing condition, 8- to 12-week-old C57BL/6-*EpCAM*$^{tml\ EpCAM}$ mice were subcutaneously injected 3×10^5 B16-EpCAM-Luc cells (B16 cell line was genetically modified to stably express human EpCAM and Luciferase). The mice were randomly divided into three groups when tumor volume reached ~15 mm^3 (about 3 days after tumor cells transfer). Three doses of murine EpCAM–CAR-T or Mock-T cells (1×10^7 per mouse) were following intravenously administrated at days 0, 3, and 7. Tumor burden was monitored by BLI, imaged with IVIS Spectrum, and analyzed using Living Image software (PerkinElmer). Murine body mass and temperature were recorded at the indicated time. The orbital blood was collected at the end of the experiment to perform a biochemistry analysis. The main organs were preserved in formalin for further analysis.

Real-time PCR

Total genomic DNA was extracted from peripheral blood samples or murine tissues using the TIANamp Genomic DNA Kit (TIANGEN). Primers were designed according to the *RRE* gene in the pCLK backbone. The following primers were used in the analysis: forward, 5′-TTTGTTCCTTGGGTTCTTGGG-3′ and reverse, 5′-GATTCTTGCCTGGAGCTGCTT-3′. Real-time PCR was performed with a SYBR Green Supermix kit (Bio-Rad) on a CFX Connect Real-Time System (Bio-Rad).

RNA sequencing

After 6 days of CAR gene modification, 1×10^6 Dectin-1, CD28, or 4-1BB CAR-T cells were stimulated for 24 hours with plate-bound antigen-Fc protein (1 μg/ml), and there were three replicates per group. The cells were collected, washed twice with PBS, and lysed with TRIzol reagent (Life Technologies). mRNA was extracted and sent to the microarray core facility of The Beijing Genomics Institute to be processed and hybridized according to the protocols specified by the manufacturers. After sequencing, clean reads were identified by DESeq2 algorithms. Further analysis was based on differentially expressed genes and visualized with the plots package in

R. Genes were considered differentially expressed if they changed more than two fold compared to the normal T cell group. GSEA was performed on different cell types in prerank list mode with 1000 permutations (nominal P value <0.01). The genes that were identified by absolute $\log_2$ fold change ≥ 1 and P value < 0.05 were considered to have significant expression changes. This experiment was repeated at least twice in the laboratory. The following T cell signature gene sets (down and up) from The Broad Institute Molecular Signature Database (MSigDB) were used: KEGG_CYTOKINE_CYTOKINE_RECEPTOR_INTERACTION, GSE23321_CENTRAL_MEMORY_VS_NAIVE_CD8_T CELL_UP_, and GSE41867_NAIVE_VS_EFFECTOR_CD8_T CELL_UP.

Histological analysis

Tumor samples and tissues were fixed in 4% paraformaldehyde overnight and then dehydrated and embedded in paraffin wax. Tissue sections were prepared for H&E staining or immunohistochemical analysis. For immunohistochemical analysis, the tissue sections were subjected to a heat-induced antigen retrieval protocol to avoid masking an epitope. The slides were incubated with 10% goat serum (ZSGB-Bio) and an endogenous peroxidase blocking agent (ZSGB-Bio) to reduce endogenous peroxidase activity and nonspecific interactions. Next, the samples were incubated with primary antibodies, including rabbit anti-CD3 (1:300; Abcam) and rabbit anti-EpCAM (1:200; Abcam). Horseradish peroxidase–labeled goat anti-rabbit immunoglobulin G (ZSGB-Bio) and DAB chromogen solution were used to produce a colored precipitate, which localized to the antigen-expressing site. If necessary, the cell nucleus was counterstained with hematoxylin. For H&E staining, xylene and ethyl alcohol were used first to remove the wax and hydrate the sections. Then, the slides were successively stained with haematoxylin and 0.5% eosin-G for 5 min. Last, the samples were cleared in purified water for 5 min. For better visual presentation, all tissue sections were scanned with Pannoramic MIDI II (3DHISTECH) and Snap using CaseViewer software (3DHISTECH).

Statistical analysis

All statistical analyses and graphs were generated by GraphPad Prism software 8.0 (GraphPad 8.0). Student's t test was used to compare the data between two groups. One-way analysis of variance (ANOVA) was performed when comparing more than two groups. Mouse survival was analyzed by using a log-rank test. The results are presented as the means ± SD unless otherwise indicated. A P value < 0.05 was considered statistically significant.

Supplementary Materials

This PDF file includes:

Figs. S1 to S10
Table S1

REFERENCES AND NOTES

1. S. J. Schuster, M. R. Bishop, C. S. Tam, E. K. Waller, P. Borchmann, J. P. McGuirk, U. Jäger, S. Jaglowski, C. Andreadis, J. R. Westin, I. Fleury, V. Bachanova, S. R. Foley, P. J. Ho, S. Mielke, J. M. Magenau, H. Holte, S. Pantano, L. B. Pacaud, R. Awasthi, J. Chu, Ö. Anak, G. Salles, R. T. Maziarz; JULIET Investigators, Tisagenlecleucel in adult relapsed or refractory diffuse large B-cell lymphoma. *N. Engl. J. Med.* **380**, 45–56 (2019).
2. E. A. Chong, M. Ruella, S. J. Schuster; Lymphoma Program Investigators at the University of Pennsylvania, Five-year outcomes for refractory B-cell lymphomas with CAR T-cell therapy. *N. Engl. J. Med.* **384**, 673–674 (2021).
3. D. L. Porter, B. L. Levine, M. Kalos, A. Bagg, C. H. June, Chimeric antigen receptor-modified T cells in chronic lymphoid leukemia. *N. Engl. J. Med.* **365**, 725–733 (2011).
4. S. Rafiq, C. S. Hackett, R. J. Brentjens, Engineering strategies to overcome the current roadblocks in CAR T cell therapy. *Nat. Rev. Clin. Oncol.* **17**, 147–167 (2020).
5. R. A. Morgan, J. C. Yang, M. Kitano, M. E. Dudley, C. M. Laurencot, S. A. Rosenberg, Case report of a serious adverse event following the administration of T cells transduced with a chimeric antigen receptor recognizing ERBB2. *Mol. Ther.* **18**, 843–851 (2010).
6. C. H. Lamers, S. Sleijfer, S. van Steenbergen, P. van Elzakker, B. van Krimpen, C. Groot, A. Vulto, M. den Bakker, E. Oosterwijk, R. Debets, J. W. Gratama, Treatment of metastatic renal cell carcinoma with CAIX CAR-engineered T cells: Clinical evaluation and management of on-target toxicity. *Mol. Ther.* **21**, 904–912 (2013).
7. C. W. Mount, R. G. Majzner, S. Sundaresh, E. P. Arnold, M. Kadapakkam, S. Haile, L. Labanieh, E. Hulleman, P. J. Woo, S. P. Rietberg, H. Vogel, M. Monje, C. L. Mackall, Potent antitumor efficacy of anti-GD2 CAR T cells in H3-K27M+ diffuse midline gliomas. *Nat. Med.* **24**, 572–579 (2018).
8. N. A. Vitanza, A. J. Johnson, A. L. Wilson, C. Brown, J. K. Yokoyama, A. Künkele, C. A. Chang, S. Rawlings-Rhea, W. Huang, K. Seidel, C. M. Albert, N. Pinto, J. Gust, L. S. Finn, J. G. Ojemann, J. Wright, R. J. Orentas, M. Baldwin, R. A. Gardner, M. C. Jensen, J. R. Park, Locoregional infusion of HER2-specific CAR T cells in children and young adults with recurrent or refractory CNS tumors: An interim analysis. *Nat. Med.* **27**, 1544–1552 (2021).
9. P. S. Adusumilli, L. Cherkassky, J. Villena-Vargas, C. Colovos, E. Servais, J. Plotkin, D. R. Jones, M. Sadelain, Regional delivery of mesothelin-targeted CAR T cell therapy generates potent and long-lasting CD4-dependent tumor immunity. *Sci. Transl. Med.* **6**, 261ra151 (2014).
10. G. Moldenhauer, F. Momburg, P. Moller, R. Schwartz, G. J. Hammerling, Epithelium-specific surface glycoprotein of Mr 34,000 is a widely distributed human carcinoma marker. *Br. J. Cancer* **56**, 714–721 (1987).
11. T. Reya, S. J. Morrison, M. F. Clarke, I. L. Weissman, Stem cells, cancer, and cancer stem cells. *Nature* **414**, 105–111 (2001).
12. M. Yu, A. Bardia, B. S. Wittner, S. L. Stott, M. E. Smas, D. T. Ting, S. J. Isakoff, J. C. Ciciliano, M. N. Wells, A. M. Shah, K. F. Concannon, M. C. Donaldson, L. V. Sequist, E. Brachtel, D. Sgroi, J. Baselga, S. Ramaswamy, M. Toner, D. A. Haber, S. Maheswaran, Circulating breast tumor cells exhibit dynamic changes in epithelial and mesenchymal composition. *Science* **339**, 580–584 (2013).
13. M. S. Khan, A. Kirkwood, T. Tsigani, J. Garcia-Hernandez, J. A. Hartley, M. E. Caplin, T. Meyer, Circulating tumor cells as prognostic markers in neuroendocrine tumors. *J. Clin. Oncol.* **31**, 365–372 (2013).
14. M. Schmidt, D. Rüttinger, M. Sebastian, C. A. Hanusch, N. Marschner, P. A. Baeuerle, A. Wolf, G. Göppel, D. Oruzio, G. Schlimok, G. G. Steger, C. Wolf, W. Eiermann, A. Lang, M. Schuler, Phase IB study of the EpCAM antibody adecatumumab combined with docetaxel in patients with EpCAM-positive relapsed or refractory advanced-stage breast cancer. *Ann. Oncol.* **23**, 2306–2313 (2012).
15. P. Wimberger, H. Gilet, A.-K. Gonschior, M. M. Heiss, M. Moehler, G. Oskay-Oezcelik, S.-E. al-Batran, B. Schmalfeldt, A. Schmittel, E. Schulze, S. L. Parsons, Deterioration in quality of life (QoL) in patients with malignant ascites: Results from a phase II/III study comparing paracentesis plus catumaxomab with paracentesis alone. *Ann. Oncol.* **23**, 1979–1985 (2012).
16. M. Kowalski, J. Guindon, L. Brazas, C. Moore, J. Entwistle, J. Cizeau, M. A. S. Jewett, G. C. MacDonald, A phase II study of oportuzumab monatox: An immunotoxin therapy for patients with noninvasive urothelial carcinoma in situ previously treated with bacillus Calmette-Guérin. *J. Urol.* **188**, 1712–1718 (2012).
17. M. Jäger, A. Schoberth, P. Ruf, J. Hess, M. Hennig, B. Schmalfeldt, P. Wimberger, M. Ströhlein, B. Theissen, M. M. Heiss, H. Lindhofer, Immunomonitoring results of a phase II/III study of malignant ascites patients treated with the trifunctional antibody catumaxomab (anti-EpCAM x anti-CD3). *Cancer Res.* **72**, 24–32 (2012).
18. Y. Yang, J. E. McCloskey, H. Yang, J. Puc, Y. Alcaina, Y. Vedvyas, A. A. Gomez Gallegos, E. Ortiz-Sánchez, E. de Stanchina, I. M. Min, E. von Hofe, M. M. Jin, Bispecific CAR T cells against EpCAM and inducible ICAM-1 overcome antigen heterogeneity and generate superior antitumor responses. *Cancer Immunol. Res.* **9**, 1158–1174 (2021).
19. K. M. Cappell, J. N. Kochenderfer, A comparison of chimeric antigen receptors containing CD28 versus 4-1BB costimulatory domains. *Nat. Rev. Clin. Oncol.* **18**, 715–727 (2021).
20. N. Singh, N. V. Frey, B. Engels, D. M. Barrett, O. Shestova, P. Ravikumar, K. D. Cummins, Y. G. Lee, R. Pajarillo, I. Chun, A. Shyu, S. L. Highfill, A. Price, L. Zhao, L. Peng, B. Granda, M. Ramones, X. M. Lu, D. A. Christian, J. Perazzelli, S. F. Lacey, N. H. Roy, J. K. Burkhardt, F. Colomb, M. Damra, M. Abdel-Mohsen, T. Liu, D. Liu, D. M. Standley, R. M. Young, J. L. Brogdon, S. A. Grupp, C. H. June, S. L. Maude, S. Gill, M. Ruella, Antigen-independent activation enhances the efficacy of 4-1BB-costimulated CD22 CAR T cells. *Nat. Med.* **27**, 842–850 (2021).

21. O. U. Kawalekar, R. S. O'Connor, J. A. Fraietta, L. Guo, S. E. McGettigan, A. D. Posey Jr., P. R. Patel, S. Guedan, J. Scholler, B. Keith, N. W. Snyder, I. A. Blair, M. C. Milone, C. H. June, Distinct signaling of coreceptors regulates specific metabolism pathways and impacts memory development in CAR T cells. *Immunity* **44**, 380–390 (2016).
22. Z. Zhao, M. Condomines, S. J. C. van der Stegen, F. Perna, C. C. Kloss, G. Gunset, J. Plotkin, M. Sadelain, Structural design of engineered costimulation determines tumor rejection kinetics and persistence of CAR T cells. *Cancer Cell* **28**, 415–428 (2015).
23. S. S. Neelapu, F. L. Locke, N. L. Bartlett, L. J. Lekakis, D. B. Miklos, C. A. Jacobson, I. Braunschweig, O. O. Oluwole, T. Siddiqi, Y. Lin, J. M. Timmerman, P. J. Stiff, J. W. Friedberg, I. W. Flinn, A. Goy, B. T. Hill, M. R. Smith, A. Deol, U. Farooq, P. McSweeney, J. Munoz, I. Avivi, J. E. Castro, J. R. Westin, J. C. Chavez, A. Ghobadi, K. V. Komanduri, R. Levy, E. D. Jacobsen, T. E. Witzig, P. Reagan, A. Bot, J. Rossi, L. Navale, Y. Jiang, J. Aycock, M. Elias, D. Chang, J. Wiezorek, W. Y. Go, Axicabtagene ciloleucel CAR T-cell therapy in refractory large B-cell lymphoma. *N. Engl. J. Med.* **377**, 2531–2544 (2017).
24. J. N. Brudno, N. Lam, D. Vanasse, Y. W. Shen, J. J. Rose, J. Rossi, A. Xue, A. Bot, N. Scholler, L. Mikkilineni, M. Roschewski, R. Dean, R. Cachau, P. Youkharibache, R. Patel, B. Hansen, D. F. Stroncek, S. A. Rosenberg, R. E. Gress, J. N. Kochenderfer, Safety and feasibility of anti-CD19 CAR T cells with fully human binding domains in patients with B-cell lymphoma. *Nat. Med.* **26**, 270–280 (2020).
25. R. A. Drummond, I. M. Dambuza, S. Vautier, J. A. Taylor, D. M. Reid, C. C. Bain, D. M. Underhill, D. Masopust, D. H. Kaplan, G. D. Brown, $CD4^+$ T-cell survival in the GI tract requires dectin-1 during fungal infection. *Mucosal Immunol.* **9**, 492–502 (2016).
26. S. Leibundgut-Landmann, F. Osorio, G. D. Brown, C. R. E. Sousa, Stimulation of dendritic cells via the dectin-1/Syk pathway allows priming of cytotoxic T-cell responses. *Blood* **112**, 4971–4980 (2008).
27. J. Chen, I. F. López-Moyado, H. Seo, C.-W. J. Lio, L. J. Hempleman, T. Sekiya, A. Yoshimura, J. P. Scott-Browne, A. Rao, NR4A transcription factors limit CAR T cell function in solid tumours. *Nature* **567**, 530–534 (2019).
28. A. Crawford, J. M. Angelosanto, C. Kao, T. A. Doering, P. M. Odorizzi, B. E. Barnett, E. J. Wherry, Molecular and transcriptional basis of $CD4^+$ T cell dysfunction during chronic infection. *Immunity* **40**, 289–302 (2014).
29. R. C. Lynn, E. W. Weber, E. Sotillo, D. Gennert, P. Xu, Z. Good, H. Anbunathan, J. Lattin, R. Jones, V. Tieu, S. Nagaraja, J. Granja, C. F. A. de Bourcy, R. Majzner, A. T. Satpathy, S. R. Quake, M. Monje, H. Y. Chang, C. L. Mackall, C-Jun overexpression in CAR T cells induces exhaustion resistance. *Nature* **576**, 293–300 (2019).
30. A. H. Long, W. M. Haso, J. F. Shern, K. M. Wanhainen, M. Murgai, M. Ingaramo, J. P. Smith, A. J. Walker, M. E. Kohler, V. R. Venkateshwara, R. N. Kaplan, G. H. Patterson, T. J. Fry, R. J. Orentas, C. L. Mackall, 4-1BB costimulation ameliorates T cell exhaustion induced by tonic signaling of chimeric antigen receptors. *Nat. Med.* **21**, 581–590 (2015).
31. L. Gattinoni, E. Lugli, Y. Ji, Z. Pos, C. M. Paulos, M. F. Quigley, J. R. Almeida, E. Gostick, Z. Yu, C. Carpenito, E. Wang, D. C. Douek, D. A. Price, C. H. June, F. M. Marincola, M. Roederer, N. P. Restifo, A human memory T cell subset with stem cell-like properties. *Nat. Med.* **17**, 1290–1297 (2011).
32. L. D. Shultz, M. A. Brehm, J. V. Garcia-Martinez, D. L. Greiner, Humanized mice for immune system investigation: Progress, promise and challenges. *Nat. Rev. Immunol.* **12**, 786–798 (2012).
33. S. S. Neelapu, S. Tummala, P. Kebriaei, W. Wierda, C. Gutierrez, F. L. Locke, K. V. Komanduri, Y. Lin, N. Jain, N. Daver, J. Westin, A. M. Gulbis, M. E. Loghin, J. F. de Groot, S. Adkins, S. E. Davis, K. Rezvani, P. Hwu, E. J. Shpall, Chimeric antigen receptor T-cell therapy - assessment and management of toxicities. *Nat. Rev. Clin. Oncol.* **15**, 47–62 (2018).
34. P. Kosti, J. W. Opzoomer, K. I. Larios-Martinez, R. Henley-Smith, C. L. Scudamore, M. Okesola, M. Y. M. Taher, D. M. Davies, T. Muliaditan, D. Larcombe-Young, N. Woodman, C. E. Gillett, S. Thavaraj, J. Maher, J. N. Arnold, Hypoxia-sensing CAR T cells provide safety and efficacy in treating solid tumors. *Cell Rep. Med.* **2**, 100227 (2021).
35. B. L. Zhang, D. Li, Y.-L. Gong, Y. Huang, D.-Y. Qin, L. Jiang, X. Liang, X. Yang, H.-F. Gou, Y.-S. Wang, Y.-Q. Wei, W. Wang, Preclinical evaluation of chimeric antigen receptor-modified T cells specific to epithelial cell adhesion molecule for treating colorectal cancer. *Hum. Gene Ther.* **30**, 402–412 (2019).
36. D. W. Lee, R. Gardner, D. L. Porter, C. U. Louis, N. Ahmed, M. Jensen, S. A. Grupp, C. L. Mackall, Current concepts in the diagnosis and management of cytokine release syndrome. *Blood* **124**, 188–195 (2014).
37. R. G. Majzner, C. L. Mackall, Clinical lessons learned from the first leg of the CAR T cell journey. *Nat. Med.* **25**, 1341–1355 (2019).
38. M. M. Heiss, P. Murawa, P. Koralewski, E. Kutarska, O. O. Kolesnik, V. V. Ivanchenko, A. S. Dudnichenko, B. Aleknaviciene, A. Razbadauskas, M. Gore, E. Ganea-Motan, T. Ciuleanu, P. Wimberger, A. Schmittel, B. Schmalfeldt, A. Burges, C. Bokemeyer, H. Lindhofer, A. Lahr, S. L. Parsons, The trifunctional antibody catumaxomab for the treatment of malignant ascites due to epithelial cancer: Results of a prospective randomized phase II/III trial. *Int. J. Cancer* **127**, 2209–2221 (2010).
39. H. Zhang, F. Li, J. Cao, X. Wang, H. Cheng, K. Qi, G. Wang, K. Xu, J. Zheng, Y.-X. Fu, X. Yang, A chimeric antigen receptor with antigen-independent OX40 signaling mediates potent antitumor activity. *Sci. Transl. Med.* **13**, eaba7308 (2021).
40. X. Liang, Y. Huang, D. Li, X. Yang, L. Jiang, W. Zhou, J. Su, N. Chen, W. Wang, Distinct functions of CAR-T cells possessing a dectin-1 intracellular signaling domain. *Gene Ther.* **30**, 411–420 (2023).
41. L. Biasco, N. Izotova, C. Rivat, S. Ghorashian, R. Richardson, A. Guvenel, R. Hough, R. Wynn, B. Popova, A. Lopes, M. Pule, A. J. Thrasher, P. J. Amrolia, Clonal expansion of T memory stem cells determines early anti-leukemic responses and long-term CAR T cell persistence in patients. *Nat. Cancer* **2**, 629–642 (2021).
42. A. I. Salter, R. G. Ivey, J. J. Kennedy, V. Voillet, A. Rajan, E. J. Alderman, U. J. Voytovich, C. Lin, D. Sommermeyer, L. Liu, J. R. Whiteaker, R. Gottardo, A. G. Paulovich, S. R. Riddell, Phosphoproteomic analysis of chimeric antigen receptor signaling reveals kinetic and quantitative differences that affect cell function. *Sci. Signal.* **11**, eaat6753 (2018).
43. X. Liu, Y. Wang, H. Lu, J. Li, X. Yan, M. Xiao, J. Hao, A. Alekseev, H. Khong, T. Chen, R. Huang, J. Wu, Q. Zhao, Q. Wu, S. Xu, X. Wang, W. Jin, S. Yu, Y. Wang, L. Wei, A. Wang, B. Zhong, L. Ni, X. Liu, R. Nurieva, L. Ye, Q. Tian, X. W. Bian, C. Dong, Genome-wide analysis identifies NR4A1 as a key mediator of T cell dysfunction. *Nature* **567**, 525–529 (2019).
44. M. Ghosn, W. Cheema, A. Zhu, J. Livschitz, M. Maybody, F. E. Boas, E. Santos, D. H. Kim, J. A. Beattie, M. Offin, V. W. Rusch, M. G. Zauderer, P. S. Adusumilli, S. B. Solomon, Image-guided interventional radiological delivery of chimeric antigen receptor (CAR) T cells for pleural malignancies in a phase I/II clinical trial. *Lung Cancer* **165**, 1–9 (2022).
45. G. Hu, G. Li, W. Wen, W. Ding, Z. Zhou, Y. Zheng, T. Huang, J. Ren, R. Chen, D. Zhu, R. He, Y. Liang, M. Luo, Case report: B7-H3 CAR-T therapy partially controls tumor growth in a basal cell carcinoma patient. *Front. Oncol.* **12**, 956593 (2022).
46. C. E. Brown, B. Badie, M. E. Barish, L. Weng, J. R. Ostberg, W. C. Chang, A. Naranjo, R. Starr, J. Wagner, C. Wright, Y. Zhai, J. R. Bading, J. A. Ressler, J. Portnow, M. D'Apuzzo, S. J. Forman, M. C. Jensen, Bioactivity and safety of IL13Rα2-redirected chimeric antigen receptor $CD8^+$ T cells in patients with recurrent glioblastoma. *Clin. Cancer Res.* **21**, 4062–4072 (2015).
47. C. E. Brown, D. Alizadeh, R. Starr, L. Weng, J. R. Wagner, A. Naranjo, J. R. Ostberg, M. S. Blanchard, J. Kilpatrick, J. Simpson, A. Kurien, S. J. Priceman, X. Wang, T. L. Harshbarger, M. D'Apuzzo, J. A. Ressler, M. C. Jensen, M. E. Barish, M. Chen, J. Portnow, S. J. Forman, B. Badie, Regression of glioblastoma after chimeric antigen receptor T-cell therapy. *N. Engl. J. Med.* **375**, 2561–2569 (2016).
48. D. Qin, D. Li, B. Zhang, Y. Chen, X. Liao, X. Li, P. B. Alexander, Y. Wang, Q.-J. Li, Potential lung attack and lethality generated by EpCAM-specific CAR-T cells in immunocompetent mouse models. *Onco. Targets. Ther.* **9**, 1806009 (2020).
49. K. Feng, Y. Liu, Y. Guo, J. Qiu, Z. Wu, H. Dai, Q. Yang, Y. Wang, W. Han, Phase I study of chimeric antigen receptor modified T cells in treating HER2-positive advanced biliary tract cancers and pancreatic cancers. *Protein Cell* **9**, 838–847 (2018).
50. S. A. Richman, S. Nunez-Cruz, B. Moghimi, L. Z. Li, Z. T. Gershenson, Z. Mourelatos, D. M. Barrett, S. A. Grupp, M. C. Milone, High-affinity GD2-specific CAR T cells induce fatal encephalitis in a preclinical neuroblastoma model. *Cancer Immunol. Res.* **6**, 36–46 (2018).
51. S. Ghorashian, A. M. Kramer, S. Onuoha, G. Wright, J. Bartram, R. Richardson, S. J. Albon, J. Casanovas-Company, F. Castro, B. Popova, K. Villanueva, J. Yeung, W. Vetharoy, A. Guvenel, P. A. Wawrzyniecka, L. Mekkaoui, G. W. K. Cheung, D. Pinner, J. Chu, G. Lucchini, J. Silva, O. Ciocarlie, A. Lazareva, S. Inglott, K. C. Gilmour, G. Ahsan, M. Ferrari, S. Manzoor, K. Champion, T. Brooks, A. Lopes, A. Hackshaw, F. Farzaneh, R. Chiesa, K. Rao, D. Bonney, S. Samarasinghe, N. Goulden, A. Vora, P. Veys, R. Hough, R. Wynn, M. A. Pule, P. J. Amrolia, Enhanced CAR T cell expansion and prolonged persistence in pediatric patients with ALL treated with a low-affinity CD19 CAR. *Nat. Med.* **25**, 1408–1414 (2019).
52. X. Liu, S. Jiang, C. Fang, S. Yang, D. Olalere, E. C. Pequignot, A. P. Cogdill, N. Li, M. Ramones, B. Granda, L. Zhou, A. Loew, R. M. Young, C. H. June, Y. Zhao, Affinity-tuned ErbB2 or EGFR chimeric antigen receptor T cells exhibit an increased therapeutic index against tumors in mice. *Cancer Res.* **75**, 3596–3607 (2015).
53. H. G. Caruso, L. V. Hurton, A. Najjar, D. Rushworth, S. Ang, S. Olivares, T. Mi, K. Switzer, H. Singh, H. Huls, D. A. Lee, A. B. Heimberger, R. E. Champlin, L. J. N. Cooper, Tuning Sensitivity of CAR to EGFR density limits recognition of normal tissue while maintaining potent antitumor activity. *Cancer Res.* **75**, 3505–3518 (2015).
54. S. A. Grupp, M. Kalos, D. Barrett, R. Aplenc, D. L. Porter, S. R. Rheingold, D. T. Teachey, A. Chew, B. Hauck, J. F. Wright, M. C. Milone, B. L. Levine, C. H. June, Chimeric antigen receptor–Modified T cells for acute lymphoid leukemia. *New Engl J Med* **368**, 1509–1518 (2013).
55. Z. Ying, X. F. Huang, X. Xiang, Y. Liu, X. Kang, Y. Song, X. Guo, H. Liu, N. Ding, T. Zhang, P. Duan, Y. Lin, W. Zheng, X. Wang, N. Lin, M. Tu, Y. Xie, C. Zhang, W. Liu, L. Deng, S. Gao, L. Ping, X. Wang, N. Zhou, J. Zhang, Y. Wang, S. Lin, M. Mamuti, X. Yu, L. Fang, S. Wang, H. Song, G. Wang, L. Jones, J. Zhu, S. Y. Chen, A safe and potent anti-CD19 CAR T cell therapy. *Nat. Med.* **25**, 947–953 (2019).
56. K. P. Micklethwaite, K. Gowrishankar, B. S. Gloss, Z. Li, J. A. Street, L. Moezzi, M. A. Mach, G. Sutrave, L. E. Clancy, D. C. Bishop, R. H. Y. Louie, C. Cai, J. Foox, M. MacKay, F. J. Sedlazeck,

P. Blombery, C. E. Mason, F. Luciani, D. J. Gottlieb, E. Blyth, Investigation of product-derived lymphoma following infusion of *piggyBac*-modified CD19 chimeric antigen receptor T cells. *Blood* **138**, 1391–1405 (2021).

57. A. Schambach, M. Morgan, B. Fehse, Two cases of T cell lymphoma following *piggyBac*-mediated CAR T cell therapy. *Mol.Ther.* **29**, 2631–2633 (2021).

Acknowledgments: We want to thank X. Yang, P. Zhang, and M. Liu for technical assistance and clinical help and advice. **Funding:** This work was supported by the National Key Research and Development Program of China (2016YFC1303403, 2020YFC0860200), the National Natural Science Foundation of China (81972878, 82172733), the Key Research and Development Program of Sichuan Province (2022ZDZX0024), and the International Cooperation Project of Sichuan Province (2021YFH0002). **Author contributions:** W.W. and Y.-Q.W. designed the whole investigation. Q.X., N.C., and J.H. designed the clinical trials. D.L., X.G., K.Y., W.Z., Y.H., X.L., J.S., L.J., J.L., M.F., Y.Y., and H.H. performed the experiments and managed the patients. J.Y., H.S., H.Y., and A.T. provided important suggestions and materials. D.L., W.Z., L.J., J.L. and J.Y. analyzed the experimental data and prepared the original manuscript. W.W. and Y.-Q. W. wrote and edited the manuscript. **Competing interests:** W.W. and Y.-Q.W. are inventors for a granted patent (CN113166274B) and two pending patents (PCT/CN2021/075544 and 202111120042.5). The authors declare that they have no other competing interests. **Data and materials availability:** All data of this study are available in the manuscript or supplementary materials. The lentivirus vectors, genetically engineered mice, and other materials used in this study are available via material transfer agreement from the corresponding author upon request.

Submitted 21 February 2023
Accepted 22 October 2023
Published 1 December 2023
10.1126/sciadv.adg9721